Forest Ecology and Management 517 (2022) 120256

Contents lists available at ScienceDirect

Forest Ecology and Management

journal homepage: www.elsevier.com/locate/foreco

Climatic sensitivities derived from tree rings improve predictions of the Forest Vegetation Simulator growth and yield model

Courtney L. Giebink [a,*], R. Justin DeRose [b], Mark Castle [c], John D. Shaw [d], Margaret E.K. Evans [a]

[a] Laboratory of Tree Ring Research, 1215 E Lowell St, Tucson, AZ 85721, USA
[b] Utah State University, Department of Wildland Resources and Ecology Center, 5230 Old Main Hill, NR 206, Logan, UT 84322, USA
[c] USDA Forest Service, Forest Management Service Center, 2150 Centre Ave Bldg A, Fort Collins, CO 80526, USA
[d] USDA Forest Service, Rocky Mountain Research Station, Forest Inventory and Analysis, 507 25th Street, Ogden, UT 84401, USA

A B S T R A C T

Forest management has the potential to contribute to the removal of greenhouse gasses from the atmosphere via carbon sequestration and storage. To identify management actions that will maximize carbon removal and storage over the long term, models are needed that accurately and realistically represent forest responses to changing climate. The most widely used growth and yield model in the United States (U.S.), the Forest Vegetation Simulator (FVS), which also forms the basis for several forest carbon calculators, does not currently include the direct effect of climate variation on tree growth. We incorporated the effects of climate on tree diameter growth by combining tree-ring data with forest inventory data to parameterize a suite of alternative models characterizing the growth of three dominant tree species in the arid and moisture-limited state of Utah. These species, *Pinus ponderosa* Dougl. ex Laws, *Pseudotsuga menziesii* var. *glauca* Mayr (Franco), and *Picea engelmannii* Parry ex Engelm., encompass the full elevational range of montane forest types. The alternative models we considered differed progressively from the current FVS large-tree diameter growth model, first by changing to an annual time step, then by adding interannual climate effects, followed by model simplification (removal of predictors), and finally, complexification, including effects of spatial variation in climate and two-way interactions between predictors. We validated diameter growth predictions from these models with independent observations, and evaluated model performance in terms of accuracy, precision, and bias. We then compared predictions of future growth made by the existing large-tree diameter growth model used in FVS, i.e., without climate effects, to those of our updated models, including those with climate effects. We found that simpler models of tree growth outperform the current FVS model, and that the incorporation of climate effects improves model performance for two out of three species, in which growth is currently overpredicted by FVS. Diameter growth projected with improved, climate-sensitive models is less than the future tree growth projected by the current climate-insensitive FVS model. Tree rings can be used to identify and incorporate drivers of growth variation into a stand-level growth and yield model, giving more accurate predictions of the carbon uptake potential of forests under climate change.

1. Introduction

Forests provide many ecosystem services, including the provisioning of timber resources, habitat for wildlife, and, importantly, climate regulation through carbon storage and sequestration. Indeed, forests are an important component of the global carbon cycle; they are estimated to be responsible for a net global sink of 1.1 ± 0.8 Pg year^{-1} of carbon (Pan et al., 2011). This critical role in the carbon cycle is recognized at an international scale, with countries planning to rely substantially upon forests to meet emissions reduction targets, in order to limit global warming to 1.5–2 °C (Grassi et al., 2017). The United States (U.S.), for example, plans to meet its target partly by enhancing its forest carbon sink through forest protection and management (The United States of America Nationally Determined Contribution, 2021). Improved forest management is recognized as a natural climate solution (Fargione et al., 2018; Griscom et al., 2017) or negative emissions technology (National Academies of Sciences, 2019). For forest management to contribute to these emission reduction targets, forest managers need scale-appropriate decision support tools to help choose between alternative management actions that might be proposed to create additional carbon sequestration or storage (i.e., additionality) over long time scales (i.e., permanence) or reduce the risk of forest carbon loss through disturbance (i.e., reversal; Giebink et al., 2022). And, importantly, these tools should take into account the impact of changing climate.

A great diversity of models can simulate forest ecosystem dynamics (Albrich et al., 2020), ranging from process-based, such as gap models (Bugmann, 2001;Shugart et al., 2018), forest landscape models (Shifley et al., 2017), dynamic global vegetation models (Fisher et al., 2018;

* Corresponding author at: USDA Forest Service, Northern Research Station, 1992 Folwell Avenue, St. Paul, MN 55108, USA; Oak Ridge Associated Universities, Oak Ridge, TN 37831, USA.
E-mail address: Courtney.Giebink@usda.gov (C.L. Giebink).

https://doi.org/10.1016/j.foreco.2022.120256
Received 2 January 2022; Received in revised form 20 April 2022; Accepted 23 April 2022
Available online 12 May 2022

Foley et al., 1996; Sitch et al., 2003), and biogeochemical models (e.g. Running and Coughlan, 1988), to empirical, such as stand-level growth and yield models (Peng, 2000; Porté and Bartelink, 2002; Weiskittel et al., 2011). These broad classes of models each have a range of complexity or realism, i.e., explicit representation of key processes, and hence key capabilities needed to anticipate forest dynamics, as well as specific areas where improvement is needed to realistically assess forest-based climate mitigation (Giebink et al., 2022). For example, forest landscape models excel at the explicit representation of spatially contagious forest processes, such as fire and insect outbreaks, which cause reversal of forest carbon stocks. Further, these models vary in terms of representation of vegetation structure, from cohort-based (e.g., LANDIS-II, Scheller et al., 2007; ED, Moorcroft et al., 2001) to individual-based (e.g., iLand, Seidl et al., 2012; SEIB-DGVM, Sato et al., 2007). The strength of empirical forestry models, in terms of anticipating and implementing forest-based climate mitigation, is their long history of development and use for site-specific forest management, and more recently, their use to estimate forest carbon stock, including life cycle analysis of carbon in wood products (Zald et al., 2016). For decades, they have undergone extensive parameterization and validation to satisfactorily represent the stand-level self-thinning process characteristic of closed-canopy forest stand development (Shifley et al., 2017; Weiskittel et al., 2011), and they have long been the simulation tool of choice used by silviculturists to make choices about forest treatments. Grounded in local observations, they have great potential to guide local-level forest management activities aimed at climate mitigation. However, they often lack representation of the influence of climate on forest dynamics and hence should be expected to extrapolate poorly to novel climate conditions (Evans, 2012).

The Forest Vegetation Simulator (FVS) is the forest growth and yield model most widely used in the U.S. (Dixon, 2002). FVS is both parameterized and initialized with regionally sourced data, often from the USDA Forest Service's Forest Inventory and Analysis (FIA) program. The FIA program was mandated in 1928 with the goal of collecting data to characterize the status and trends of forested lands in the U.S., and hence its sampling was designed to be representative of the range of forest conditions in each state (Burrill et al., 2018). There are 22 regional FVS variants that use tree-level and plot-level inventory data to simulate the response of a forest stand to silvicultural treatments, such as thinning, or other perturbations, such as prescribed fire (Crookston and Dixon, 2005), making the expected consequences of different management actions easy to compare in a multiple scenario framework, as required by the National Environmental Policy Act. Here, we focus on the central growth component of FVS, the large-tree diameter growth model, because it strongly influences stand development in simulations (Dixon, 2002), and it relates directly to carbon sequestration. Indeed, FVS is used in several forest carbon calculators (Zald et al., 2016) and is an approved empirical model by several carbon accounting protocols, including the California Air Resources Board, for estimating baseline carbon stocks and projecting selected carbon pools (California Air Resources Board, 2015).

Relatively recently, it became possible to evaluate climate change impacts in FVS with an extension called Climate-FVS (Crookston et al., 2010). Climate-FVS has several options for incorporating the effect of changing climate on tree growth. The first uses estimates of climatic suitability derived from species-level environmental envelopes (e.g., Rehfeldt et al., 2006) to modify expected tree growth. That is, climate responses are determined by modeling data on a species' occurrence as a function of climate. However, evidence has accumulated, including from studies of trees based on forest inventory and tree-ring data, that the climate optimum for occurrence or abundance is frequently not the same as the optimum for underlying vital rates like growth (Bohner and Diez, 2019; McGill, 2012; Pagel et al., 2020; Pironon et al., 2018; Thuiller et al., 2014). Hence, occurrence data may not be the best way to anticipate how individual tree growth will respond to shifting climate. The second option in Climate-FVS is to modify tree growth based on population-level climate responses estimated from provenance tests (Leites et al., 2012), which are ideal for separating genetic vs. plastic responses (Aitken and Bemmels, 2016; Alberto et al., 2013; Housset et al., 2018; Langlet, 1971). These response functions are based on the cumulative growth of trees a certain number of years after they were planted, in response to the climate that they experience at the common garden location (Leites et al., 2012), i.e., average growth in response to average climate, and how that varies among provenances. Climate-FVS then applies these climate responses, inferred from provenance data on just two species, which are categorized as a climate specialist and a climate generalist, to other species according to their climatic niche breadth, when it is known. Species for which climatic niche breadth is unknown are assumed to never become limited by maladaptation to climate (Crookston et al., 2010). This modification is a coarse representation of plastic responses to average climate conditions.

An alternative approach to model the effect of climate variation on individual tree growth is to use the response to climate variability recorded in annual growth rings (Martin-Benito et al., 2011). Tree rings sampled at a broad spatial scale or across gradients can be used to quantify intraspecific (population-level) heterogeneity in average growth rate and the sensitivity of growth to interannual climate variability (Canham et al., 2018; Klesse et al., 2020; McCullough et al., 2017).That is, tree rings offer an empirical way to estimate species-specific responses to temporal as well as spatial variability in climate. Tree cores are collected easily and without harm to the tree with an increment borer, a tool that was invented by a forester with both practical and scientific intent, i.e., to explore environmental influences on tree growth (Somerville, 1891). However, this original intent has been far from fully realized in forest management. Instead, the use of tree-ring data has largely been limited to estimating recent 5- or 10-yr diameter increment and stand age.

We fill this gap by using the information contained in ring-width data on an individual tree's response to interannual variation in climate to incorporate climate sensitivity into FVS. Increment cores sampled in FIA's network of permanent sample plots throughout the interior western U.S. were recently compiled into a tree-ring data network (DeRose et al., 2017). This unbiased FIA tree-ring data set (Klesse et al., 2018) presents a unique opportunity to use the rich information on climate effects recorded in annual growth rings, complemented by inventory data from their associated forest plots, to parameterize FVS growth models. This combination of tree-ring and forest inventory data makes it possible not only to build a climate-sensitive version of FVS, but also to look more closely at the representation of tree growth in FVS, including alternative combinations of predictors of tree growth, and how climate might interact with other drivers (e.g., competition, tree size).

Hence our aim was to build a climate-sensitive and appropriately complex version of the large-tree diameter growth model currently used in FVS, based on tree-ring and forest inventory data. With this goal in mind, we created a suite of alternative models for three dominant species in Utah and asked: 1) what are the important drivers of growth variation estimated from tree-ring and forest inventory data? 2) Does the use of tree-ring data and climate effects improve model performance in terms of the accuracy, precision, and bias of growth predictions, using out-of-sample observations? And which among several different model structures performs best at predicting tree growth? Finally, 3) if model performance is improved with an alternative model structure, under changing climate, how does expected future growth, and by extension, carbon sequestration, differ from expected growth based on the current FVS model without climate effects? With this, we take a step towards better anticipation of the carbon sequestration potential of forest ecosystems experiencing changing climate.

2. Materials and methods

2.1. Growth & yield model

Of the regional variants of FVS, we chose to focus on the Utah variant (Keyser and Dixon, 2019) because of the authors' collective familiarity with this variant and region (DeRose et al., 2011), and the availability of tree-ring data associated with FIA data (DeRose et al., 2017). In the Utah variant, the base large-tree (>3 in. [in], or > 7.62 cm [cm]) diameter growth model is a multiple regression with the following terms:

$$\ln(dds) = b_1 + b_2 * SICOND + b_3 * \sin(ASP\text{-}0.7854)*SL + b_4 * \cos(ASP\text{-}0.7854)*SL + b_5 * SL + b_6 * SL^2 + b_7 * \ln(DBH) + b_8 * (BAL/100) + b_9 * CR + b_{10} * CR^2 + b_{11} * DBH^2 + b_{12} * PCCF + b_{13} * (CCF/100) \quad (1)$$

Where dds is 10-year predicted change in squared inside-bark diameter (modeled as in^2 in FVS, but shown here in cm^2; Dixon, 2002), and b_x are the estimated effects (regression coefficients) of each predictor, or covariate, with b_1 an adjustment based on forest location, and b_2 an adjustment based on the dominant species in the stand. The predictors in this model fall into three categories: site-level biophysical, tree-level, and competition variables (Table 1).

2.2. Data

We recalibrated the base FVS large-tree diameter growth model (Eq. (1)) using tree-ring data (Giebink 2022) that are part of a recently developed data network sourced in FIA plots across the U. S. Interior West region (DeRose et al., 2017), as well as tree- and plot-level data derived from the FIA DataMart (Forest Inventory and Analysis Database). Tree-ring data were linked to FIA data with a unique tree identifier (i.e., TRE_CN; Burrill et al., 2018). The data used in model calibration were collected during periodic inventories in Utah before 1999, mostly between 1988 and 1995, while model validation and projection of future tree growth used FIA data collected after the passage of the 1998 Farm Bill, which mandated a standardized sampling approach and annual data collection nationwide. Increment cores were taken from tree species with a majority representation on the plot in terms of stocking (Arner et al., 2001). Ring-width time series were developed from increment cores by repreparing the samples, cross-dating, and measuring ring widths according to standard dendrochronology protocol (DeRose et al., 2017; Speer, 2010).

We parameterized species-specific growth models for the three most abundant tree species in the Utah portion of the tree-ring data network: Douglas-fir (*Pseudotsuga menziesii* var. *glauca* Franco) (number of trees with cores [n] = 111), ponderosa pine (*Pinus ponderosa* Douglas ex P. Lawson & C. Lawson) (n = 69), and Engelmann spruce (*Picea engelmannii* Parry ex Engelm.) (n = 85). These species encompass the full elevational gradient of montane forests in Utah (Supplementary Fig. 1). In the arid state of Utah, trees are generally assumed to be moisture-limited, with positive precipitation sensitivity and negative temperature sensitivity (DeRose et al., 2013). The sampled trees are evenly distributed across forested land in Utah, with the exception of drought-tolerant ponderosa pine, which is concentrated in the southern region of Utah. Most trees were on plots with no visible disturbance (i.e., the disturbance code [DISTRBCD1] from the condition [COND] table of the FIA database was 0 or NA for 84 of the 111 [75.7%] Douglas-fir, 56 of the 69 [81.2%] ponderosa pine, and 67 of the 85 [78.8%] Engelmann spruce; Supplementary Fig. 2), after which fire damage was the most prevalent disturbance recorded (15.3% of Douglas-fir, 8.7% of ponderosa pine, and 9.4% of Engelmann spruce; Burrill et al. 2018). Most trees were on plots with no observable treatment (i.e., the treatment code [TRTCD1] from the condition table of the FIA database was NA for 82.9% of the Douglas-fir and 65.9% of the Engelmann spruce), with the exception of a high proportion of cutting observed on plots with ponderosa pine (68.1%; Supplementary Fig. 2).

Climate data at 4-km resolution were downloaded from the PRISM Climate Group (Daly et al., 2008). Historical (1895–1980) and recent (1981-present) monthly total precipitation (mm), minimum average temperature (°C), and maximum average temperature (°C) were obtained from January 1985 to May 2020. Mean annual precipitation (mm) and mean annual temperature (°C) covering the period 1981 to 2010 were obtained as climate normals, and represent average climate

Table 1
Predictors in the diameter growth models. Each variable is listed with a description, units, and data source, either the FIA database or derived from it.

Acronym	Name	Type	Description	Source
SICOND	Site index	Site-level biophysical	Average height in feet the site species (SISP*) is expected to attain in well-stocked, even-aged stands at a specified base age (SIBASE**), measure of site quality (Monserud, 1984)	FIA Condition Table
SL	Slope angle	Site-level biophysical	To the nearest 1 percent	FIA Condition Table
sin(ASP-0.7854) *SL	Solar radiation	Site-level biophysical	Radiation by eastness	Calculated; aspect (ASP) obtained from FIA Condition Table
cos(ASP-0.7854) *SL	Solar radiation	Site-level biophysical	Radiation by northness	Calculated; aspect (ASP) obtained from FIA Condition Table
DBH	Diameter at breast height	Tree-level	Bole measured in inches at 1.3 m above ground	FIA Tree Table
BAL	Basal area of live trees larger than the subject tree	Competition	Measure of absolute competition from above in square feet per acre	Calculated from DBH
CR	Compacted crown ratio	Tree-level	Percentage (0–100) of the height of a tree with live foliage, metric of tree vigor	FIA TREE Table; change is calculated using the Weibull distribution (Dixon, 1985)
PCCF	Crown competition factor on the subplot	Competition	Measure of relative competition on the subplot expressed as percentage per acre	Calculated as the summation of individual tree crown competition factor (Keyser and Dixon, 2019; Krajicek et al., 1961)
CCF	Stand crown competition factor	Competition	Measure of relative competition expressed as percentage per acre	Calculated as the summation of individual tree crown competition factor (Keyser and Dixon, 2019; Krajicek et al., 1961)
SDI	Stand density index	Competition	Measure of stand stocking, trees per acre at a 25 cm DBH index	Calculated using the summation method (Shaw, 2006)

* In most cases, SISP will be one of the species that define the forest type of the condition. In cases where there are no suitable site trees of the type species, other suitable species may be used (Burrill et al., 2018).
** The SIBASE of the site index curve used to derive site index is typically 50 or 100 years (Burrill et al., 2018).

conditions. We used the online archive of Downscaled Coupled Model Intercomparison Project (CMIP) 3 and CMIP5 Climate and Hydrology Projections (https://gdo-dcp.ucllnl.org/downscaled_cmip_projections) to obtain future climate from an ensemble of CMIP5 climate models. Specifically, we downloaded the BCSD-CMIP5-Hydrology projections of monthly precipitation (mm) and maximum temperature (℃) at $^{1}/_{8}$ degree resolution (approximately 12 km by 12 km) for all available climate models and representative concentration pathways (RCP, Reclamation, 2014). Climate data were extracted for each tree using FIA plot-level latitude and longitude coordinates (Burrill et al., 2018). To protect forest landowners, latitude and longitude coordinates that are available to the public are truncated, or 'fuzzed,' but are assumed to be within one kilometer of actual locations (Tinkham et al., 2018).

2.3. Calibration

2.3.1. Annualization of focal tree size using tree rings

The first step towards incorporating climate data into the large-tree diameter growth model was the annualization of the data used to calibrate the model - that is, converting the time step the model operates on from ten years to one year - starting with tree size (diameter at breast height, DBH; Fig. 1). For trees from which increment cores were collected, DBH was obtained for the year of measurement (Table 1) and back-calculated using the ring-width data. To calculate DBH of the previous year, diameter increment (two times the width of the annual growth ring), adjusted by a species-specific bark growth factor (Keyser and Dixon, 2019), was subtracted from the DBH measurement (Dixon, 2002). This process was repeated to back-calculate DBH each year for 30 years or until the first year of ring-width measurements, whichever came first. We chose to truncate the time series at a maximum of 30 years as a compromise between maximizing the information on climate

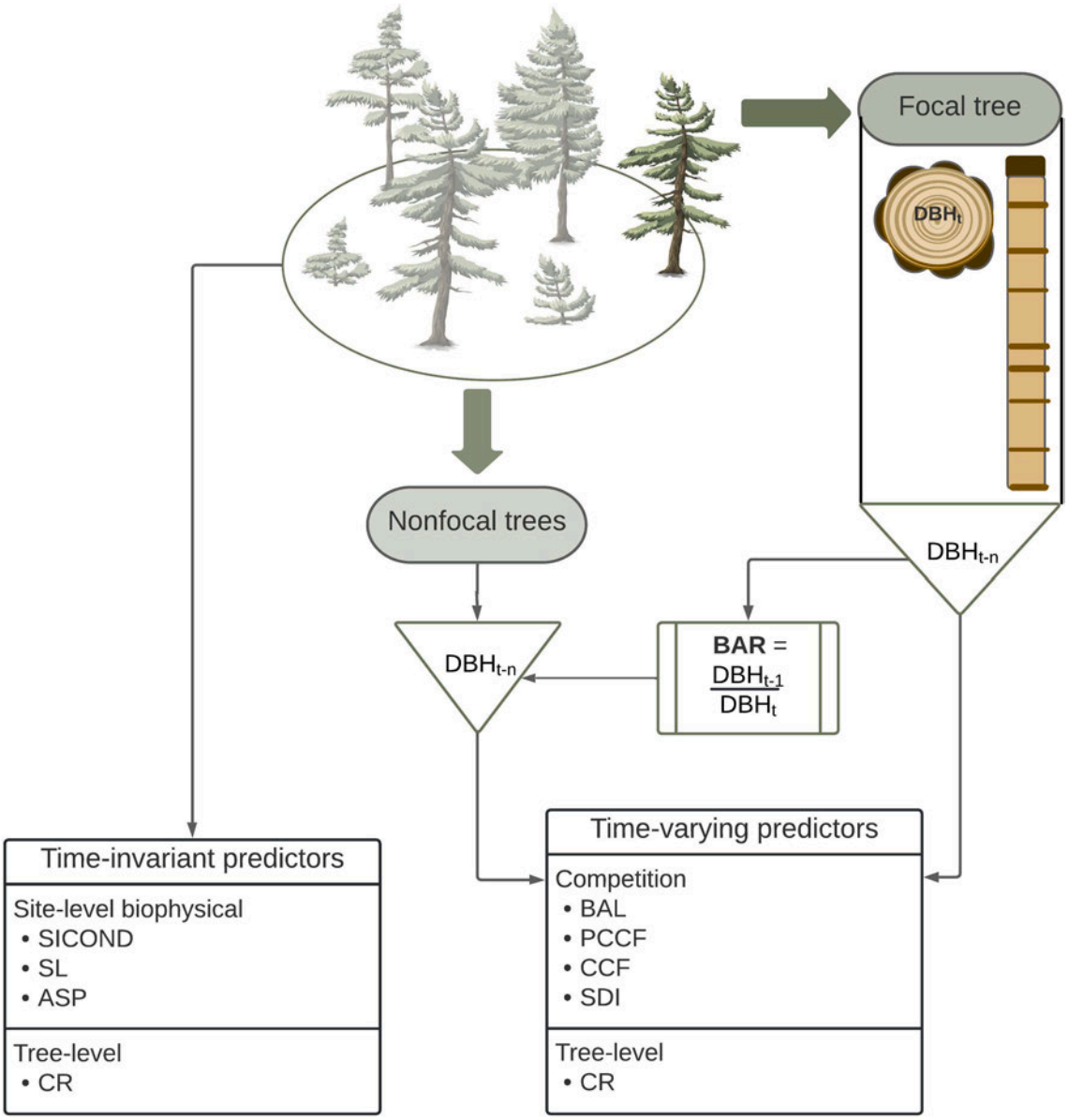

Fig. 1. Procedure for creating the calibration dataset. Each forest plot (top) consists of focal trees, from which increment cores were sampled, and nonfocal trees, without increment cores. Tree ring measurements and field-measured diameter at breast height (DBH) were used to back-calculate DBH, which was then used to estimate the basal area ratio (BAR). Average BAR was then used to back-calculate DBH for nonfocal trees. Back-calculated DBH for both focal and nonfocal trees were then used to estimate time-varying predictors, whereas time-invariant predictors were taken directly from the FIA database.

responses and minimizing the increasing uncertainty associated with reconstructing past forest conditions, such as the competitive environment (sometimes referred to as the "fading record", Swetnam et al., 1999).

2.3.2. Back-calculation of time-varying predictors of growth

In order to back-calculate dynamic (time-varying) predictors of tree growth for each year, annual DBH was needed for every tree on a plot, including trees that were not sampled for tree rings. Trees without increment cores, which contribute to the competitive environment by their presence on the plot, are referred to as "nonfocal" trees. To back-calculate DBH for nonfocal trees, we applied the basal area ratio (BAR) method (Dixon, 2002; Fig. 1). We estimated annual BAR specific to our dataset by calculating BAR for each pair of years for each tree with an increment core. We then assigned an average BAR to each nonfocal tree, first based on matching plot and species, then species, and finally, an average across all plots and species. Average BAR was then used to back-calculate DBH every year for nonfocal trees.

With back-calculated values of DBH for all trees on a plot, we annualized the competition variables (Fig. 1), which included total basal area of live trees larger than the focal tree (BAL), crown competition factor on a subplot (PCCF), and crown competition factor on a plot (CCF, Table 1). In addition, we calculated time-varying stand density index (SDI) using the summation method (Shaw, 2000; Stage, 1968).

Which trees were included in the calculation of BAL, PCCF, CCF, and SDI depended on the sampling design. Most trees in the calibration data set were sampled on plots using a variable-radius design. Consistent with this variable-radius design, we dropped trees from the data set if their distance from the sampling point was larger than the limiting distance for a tree of that diameter and updated the expansion factor, i.e., trees per acre (TPA, Burrill et al., 2018). On fixed-radius plots, all trees were retained and TPA was constant over time.

A final step in the back-calculation of the competitive environment was to explicitly account for recently dead trees, which were assumed to have died in the 10 years before plot measurement (US Department of Agriculture, 2020). These trees were randomly assigned a mortality year from zero to 9 years prior to the measurement year and included in the calculation of competition metrics in the years prior to their death.

Compacted crown ratio (CR) should change over time as a tree increases in height and the surrounding competitive environment changes. CR was obtained (Table 1) for the measurement year and back-calculated using the Weibull distribution method described by Dixon (1985). CR change was constrained to one percent per year, as it is in FVS, to avoid large changes (Keyser and Dixon, 2019).

2.3.3. Time-invariant predictors of growth

We treated site-level biophysical variables, including slope (SL), radiation terms (i.e., sin(ASP–0.7854)* SL and cos(ASP–0.7854)* SL), and site index (SICOND), as constant over time. We also fit growth models with CR treated as constant because we found poor correspondence between forward-calculated CR and observations of CR at remeasurement (Supplementary Fig. 3).

2.3.4. Calculation of tree growth

We calculated annual dds (cm^2) from ring width (mm) observations (Dixon, 2002; Stage, 1973). Missing values in the calibration data set were either corrected or the observation was removed. Missing rings (i.e., ring width is zero) were replaced with the smallest ring-width measurement for that tree, to avoid taking the log of zero in regression models and as an alternative to choosing an arbitrarily small number to add to all observations. SICOND was corrected when site species (SISP) did not match the species of the tree being modeled. This correction was done by cross matching plots from the periodic to annual design and extracting the appropriate SICOND for the species.

2.3.5. Model building - a series of tests

We fit a series of regression models for each species to systematically test whether updates to the base FVS large-tree diameter growth model (Eq. (1)) improve model prediction (Fig. 2). The first was parameterized using the tree-ring data and included all terms in the species-specific base FVS model (i.e., Full Annual model). The second added the direct effect of interannual climate variation on diameter growth (i.e., Full Climate model). Hence the former tested the effect of annualizing growth with tree rings, while the latter tested the effect of incorporating climate sensitivities recorded in tree rings. We then tested models of reduced complexity through stepwise removal of non-significant terms in Eq. (1) (i.e., Reduced Annual and Reduced Climate models). Finally, we added complexity to the Reduced Climate model, including spatial variation in climate as a 30-year average (i.e., Climate Normals model), and two-way interactions (i.e, Normals + Interactions model) between terms. As in the large-tree diameter growth model currently used in FVS (Eq. (1)), all the models are multiple linear regressions that predict tree growth as a function of covariates. Below we first describe details that were common across all models, followed by details that are specific to certain models.

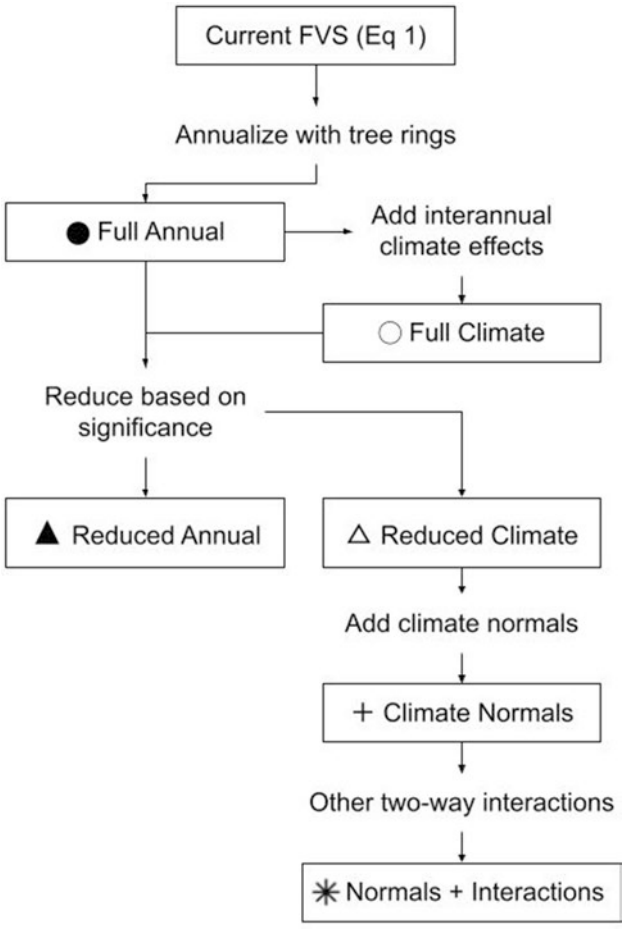

Fig. 2. Alternative diameter growth models progressively diverged from the current large-tree diameter growth model in FVS (which is shown in Eq. (1)). First, tree rings were used to convert the model to a one-year time step (annualization), creating the Full Annual model. Second, interannually varying climate variables were added as predictors, creating the Full Climate model. Third, Full models were reduced based on significance, creating the Reduced Annual and Reduced Climate models. From the Reduced Climate model, the Climate Normals model was created by adding climate normals (i.e., 30-year average) as a predictor and their significant interactions with interannual climate predictors, which was then used to create the Normals + Interactions model by adding all other significant two-way interactions.

The response variable in the regression models was log-transformed to correct for right skew. Although a generalized linear (mixed) model with a gamma distribution and a log link is often used to satisfy the assumption of normality for positive, right-skewed data, we used a linear (mixed) modeling of log-transformed dds to ease integration of model output into FVS. In addition, residual analysis showed no improvement in a model with a gamma distribution and log link. Covariates were globally standardized by mean-centering and dividing by standard deviation, which facilitates model convergence and allows model coefficients to be interpreted as standardized effect sizes (Schielzeth, 2010). In order to standardize DBH and compare its effect against other predictors, we did not log-transform DBH (diverging from Eq. (1)).

To account for correlation or clustering within the data set, we used linear mixed effects models, implemented in the R package lme4 (Bates et al., 2015). A random tree effect was tested to account for variation among trees in average growth rate (dds), and a random effect on DBH was tested to account for variation among trees in the size-related growth decline in growth ring widths. That is, with increasing tree size, ring widths generally decrease as growth is spread out over an increasingly larger circumference (even though larger trees actually grow more than smaller trees in absolute terms; Bowman et al., 2013). A random year effect tested for systematic variation in growth rate among years not accounted for by climate predictors. Tree random effects were not nested within plot random effects because there was little to no replication of trees sampled for tree rings per plot. Tree random effects nested within forest location random effects, which are based on national forest boundaries (Keyser and Dixon, 2019), were tested as an analog of the location intercept adjustment in the base FVS model (b_1 in Eq. (1)). We tested random effect structures with likelihood ratio tests. Model fit was further assessed for fixed effects using Akaike information criterion (AIC, Akaike, 1974).

These mixed effects models take the general form:

$$Y = X\beta + Z\mu + \varepsilon \quad (2)$$

Where, Y is a vector of responses (ln(dds)), X is a matrix of predictor variables, β is a vector of the fixed-effects regression coefficients, Z is a matrix of the random effects and groups (DBH, tree, year), μ is vector of the random effects, and ε is a vector of residuals.

2.3.6. Alternative growth models

Compared to the Full Annual model, the first set of species-specific alternative models differ by including climate data (i.e., Full Climate). For each species, we identified monthly and seasonal precipitation and temperature variables that significantly influenced growth using response function analyses in the R packages dplR (Bunn, 2008) and treeclim (Zang and Biondi, 2015). Our strategy for selecting climate variables differed between precipitation and temperature. Because of high uncertainty among climate models with respect to projected future precipitation, we preferred the use of precipitation variables covering a longer rather than a shorter time window. While preliminary analyses indicated seasonal precipitation variables had higher correlations with ring-width variability and inclusion of these terms yielded lower AIC scores in regressions, we chose to use total precipitation over a 16-month period for all species as a predictor in the diameter growth model, with the idea that this may make predictions of future growth more robust in response to changes in the timing of precipitation. Specifically, we chose a 16-month period that included the previous and current growing season, from previous June to current September, to account for significant lagged climate effects. In contrast, projected future temperature has lower uncertainty, so we chose to use the monthly or seasonal temperature variables that most strongly correlated with ring-width variability and gave the lowest AIC.

From these two groups of full-complexity models (Full Annual and Full Climate), we then created the Reduced Annual and Reduced Climate models. We eliminated covariates in Eq. (1) based on a lack of significance at the $p = 0.05$ level (R package lmerTest, Kuznetsova et al., 2017) and patterns of collinearity determined by variance inflation factor (VIF) with a threshold of 3 (R package car, Fox and Weisberg, 2019), since the inclusion of multiple, collinear predictors can make model inference unstable (Dormann et al., 2013). We retained at least one competition predictor based on AIC score, even if it was insignificant at the $p = 0.05$ level, because we considered the density-dependent regulation of growth necessary to capture forest stand development. In addition to the three competition variables in Eq. (1) (BAL, PCCF, and CCF), we tested SDI as a fourth alternative predictor. Finally, models with constant CR were tested. Based on AIC score, several reduced model versions for each species were chosen to test in validation. However, for ponderosa pine, it was difficult to estimate effects given a small sample size, so we further tested statistically nonsignificant predictors, including SICOND and SL, and required the sign of the single competition coefficient retained to be negative.

We then explored models with greater complexity. First, we added 30-year mean annual precipitation and mean annual temperature (i.e., climate normals), creating the Climate Normals model, to examine whether spatial variation in mean annual precipitation and temperature affect growth. The Climate Normals model also included two-way interactions between climate normals and the time-varying climate predictors, to evaluate possible spatial variation in climate sensitivity. Second, we tested all two-way interactions, building the Normals + Interactions model. The final forms of all reduced model versions were chosen after checking model performance through validation.

2.4. Validation

We performed out-of-sample validation (Cawrse et al., 2010) by comparing observed diameter growth against predicted diameter growth in trees independent of the calibration data. Trees used in validation were selected from the FIA database for the state of Utah based on the following criteria: they had to be alive at two sequential measurements, larger at the remeasurement, and on forested plots with just one forest condition. Under these criteria, Douglas-fir (n = 891), ponderosa pine (n = 384), and Engelmann spruce (n = 1144) trees selected were from the annualized (post-1999) design, which has a standardized fixed-radius sample plot design.

All covariate data were obtained or calculated following the procedures used to create the calibration data set, except DBH of nonfocal trees. Linear interpolation between the first and second measurement was used to annualize DBH of nonfocal trees. If a tree died between the two measurements, diameter was linearly interpolated between the first measurement and the estimated year of death.

Growth of all focal trees was simulated from the initial measurement year to the remeasurement year using only the fixed effects in the alternative species-specific models created from the calibration data, including models with either constant or time-varying CR. We compared model-predicted diameter growth against observed diameter growth (~10-yr diameter increment) for all the tree-ring based model versions as well as the current FVS large-tree diameter growth model, which we established as a baseline for model performance. Model performance was quantified using three metrics derived from a regression of observed vs. predicted (Piñeiro et al., 2008) diameter increment: adjusted R squared (R^2), root mean square error (RMSE), and slope of the linear model. We chose a subset of the models that produced optimal values of these performance metrics for the next step, projection of tree growth under future climate.

2.5. Projection

Trees selected from the FIA database for projection of tree growth included Douglas-fir (n = 995), ponderosa pine (n = 460), and Engelmann spruce (n = 1340) in Utah from the most recent inventory,

measured in 2010 or after, and were alive and on forested plots with just one condition.

Growth was projected using four high-performing growth models: Reduced Annual, Reduced Climate, Climate Normals, and Normals + Interactions (Fig. 2). We stopped growth projections at 2060 due to the computational toll of repeated projection cycles. All covariates were obtained from the FIA database or calculated as in validation, except the DBH of nonfocal trees and climate data. Growth of nonfocal trees was projected with FVS using 5-year projection cycles to leverage the output provided by FVS. This information was then annualized using linear interpolation. Projections in the Utah variant of FVS included mortality, which is distributed across the expansion factor (i.e., TPA) of each tree in a stand. TPA was updated every year by linearly interpolating TPA output from FVS. In the models that included interannually varying climate as a predictor of growth, i.e., Reduced Climate, Climate Normals, Normals + Interactions models, PRISM data were used for years before 2020, whereas beginning with the year 2020 (and after), downscaled projections of future climate (Supplementary Table 1, Reclamation 2014) were used. In total, these models used output from 50 different combinations of a general circulation model (GCM) and emissions scenario: 21 GCM projections under the "green world" scenario of RCP2.6 and 29 GCM projections under the "business as usual" scenario of RCP8.5. In the Climate Normals and Normals + Interactions models, the 30-year average from 1981 to 2010 climate predictors (i.e., climate normals) were carried through projection to avoid space-for-time substitution (Klesse et al. 2020).

We then used two methods to compare relative growth rate for each tree predicted by the four updated growth models (i.e., Reduced Annual, Reduced Climate, Climate Normals, and Normals + Interactions) against growth predicted by the current FVS large-tree diameter growth model. The first comparison was a paired-sample *t*-test to estimate the mean difference in cumulative growth for each updated growth model, GCM, and RCP combination (Fig. 3). Second, to examine differences in relative growth rate related to tree size, we used a paired-sample *t*-test to estimate the mean difference in cumulative growth for seven 5-inch diameter classes from 3 to 38 in. for each updated growth model, GCM, and RCP combination. In both methods, we filtered for significant differences ($p < 0.05$) and further calculated the average difference across GCMs for each emissions scenario (RCP2.6 or RCP8.5) for the Reduced Climate, Climate Normals, and Normals + Interactions models.

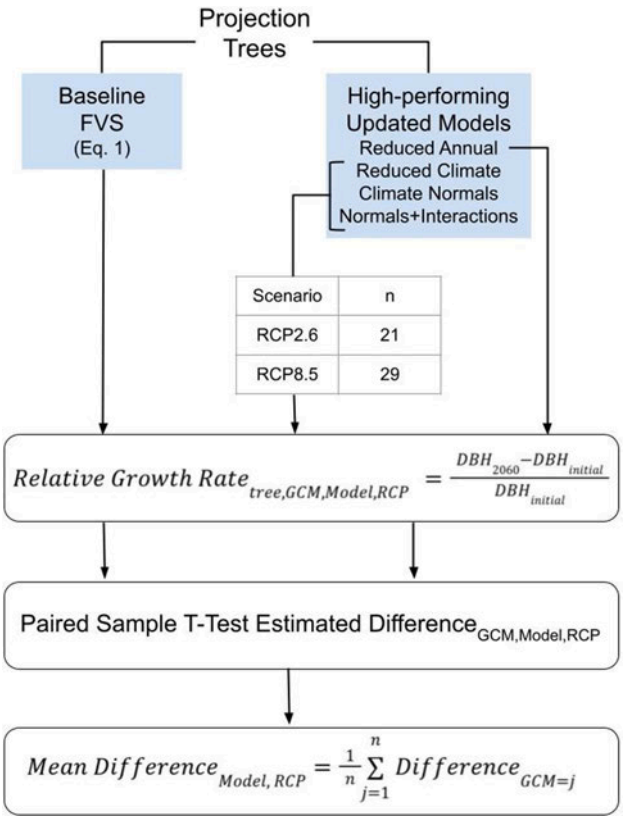

Fig. 3. Procedure for comparing tree growth projected (~2010–2060) by the baseline Forest Vegetation Simulator (FVS) against high-performing, updated diameter growth models parameterized with tree-ring data. The growth of a set of trees selected from the FIA database was simulated using both the baseline FVS model (Eq. (1)) and each of the updated models listed (Reduced Annual, Reduced Climate, Climate Normals, or Normals + Interactions), using global circulation model (GCM) and climate scenario (either RCP2.6 or RCP8.5) combinations listed in Supplementary Table 1. At the end of the projection period, each tree's relative growth rate (RGR) was calculated for each combination of model, GCM, and RCP. A paired sample *t*-test was used to estimate the average difference in projected growth between FVS and the output of each updated model, GCM, and RCP combination. These estimated differences were used to calculate the mean difference across GCMs for each model and RCP scenario.

3. Results

3.1. Calibration

We fit a series of alternative growth models for each species (Fig. 2). All models, across species, were best fit with the same random effects structure. Likelihood ratio tests failed to reject models with a random intercept for each year and a random effect for each tree on the intercept and the slope of DBH ($p < 0.001$). The addition of a random intercept for each tree nested within a forest, which is analogous to FVS's use of forest location code to modify average growth, did not consistently improve model fit to data across species.

Response function analyses revealed that precipitation was most strongly correlated with ring-width index, especially previous summer and current summer precipitation across species (Supplementary Figs. 4-6). Additionally, significant correlations were positive for precipitation variables and negative for temperature variables across species. The temperature predictor that resulted in the lowest AIC score was average maximum monthly temperature from February to July for Douglas-fir, average maximum monthly temperature from June to August for ponderosa pine, and maximum temperature of the previous August for Engelmann spruce.

Collinearity among covariates was limited (VIF < 3.0); hence, none were dropped for this reason. Instead, we kept covariates in reduced-complexity models based on statistical significance (alpha = 0.05) for explaining variation in growth and performance in validation. Competition covariates (BAL, CCF, PCCF, SDI) did not consistently explain variation in growth across species (Figs. 4a, 5a and 6a). While the current species-specific FVS models include more than one competition parameter, we kept one competition variable for each species-specific model parameterized with tree-ring data, which was sufficient to explain the negative effect of competition. We dropped the northness and eastness radiation terms because their effects were not significant and were inconsistent across species.

With standardized predictors across models, effect sizes were based on the magnitude of the coefficient (Schielzeth, 2010). In all models, DBH had the largest effect on diameter growth (Figs. 4a, 5a and 6a). A positive effect of the linear term and a negative effect of the quadratic term indicated that at the smallest DBH values, diameter increment increases with increasing DBH, whereas at larger values of DBH, diameter increment declines with increasing DBH. Across all three species, the effect of precipitation on growth was positive, whereas the effect of temperature was negative, as expected. In addition, the interaction between interannual precipitation and temperature was positive, implying that a higher value of one resulted in a greater, more positive effect of the other (Figs. 4b, 5b and 6b). Variables describing competitive pressure (BAL, CCF, SDI) had the smallest effect for all species (Figs. 4a, 5a

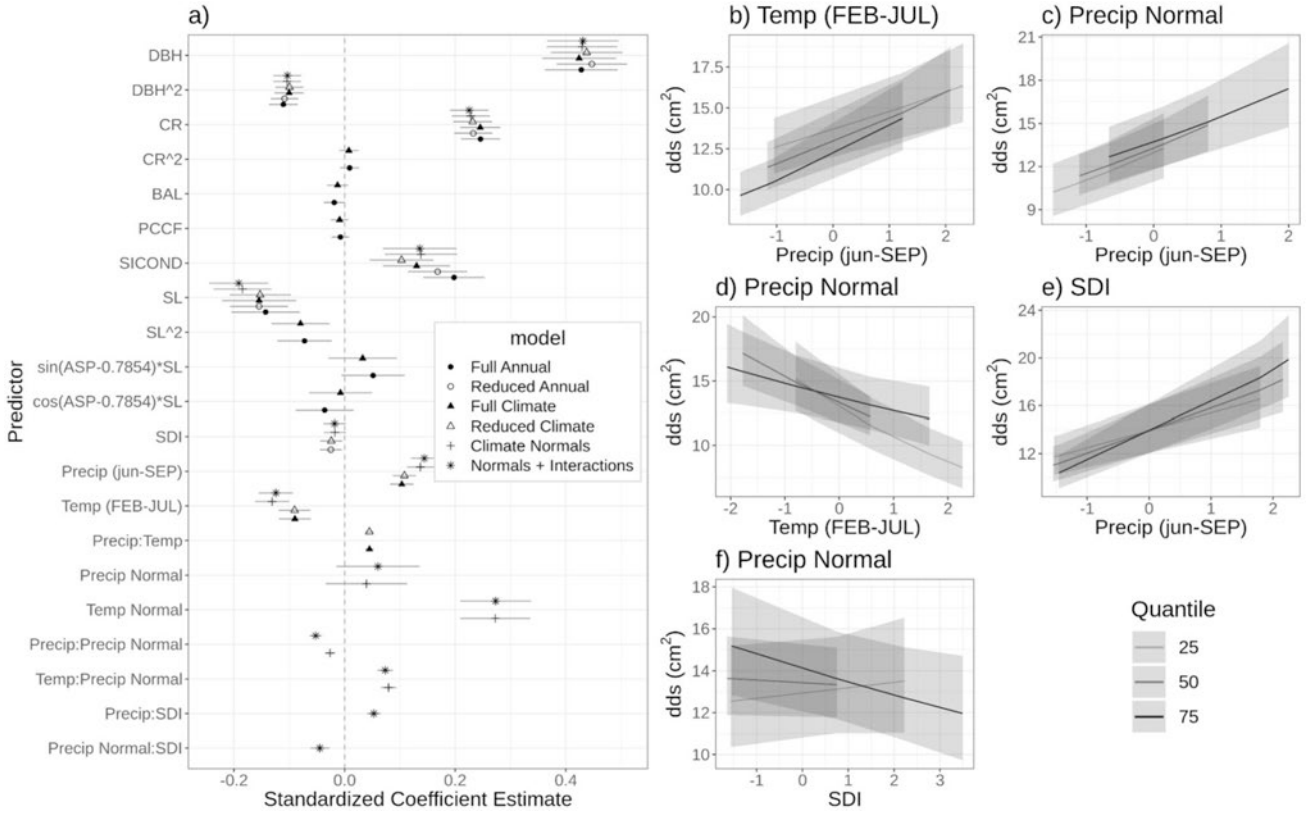

Fig. 4. Estimates of effects from Douglas-fir growth models. Standardized regression coefficients and their standard errors are shown in (a) for the predictors in all six models described in Fig. 2 and the text. Marginal effects of interaction terms on the growth response (dds) are shown, including the interaction between interannually varying precipitation (i.e., total precipitation [Precip] from previous June to current September [jun-SEP]) and interannually varying temperature (i.e., mean monthly max temperature [Temp] from current February to July [FEB-JUL]) (b), Precip (jun-SEP) and normal precipitation (Precip Normal) (c), Temp (FEB-JUL) and Precip Normal (d), Precip (jun-SEP) and stand density index (SDI) (e), and SDI and Precip Normal (f). Each of these panels shows one main effect (on the x-axis) conditional on the 25th, 50th, and 75th quantile of the other main effect (indicated in the panel title) with a 95% confidence interval around the prediction. Predicted effects are only plotted for known observations falling within the 95% confidence interval of the quantile.

and 6a). While interannual climate and competition had small effect sizes, they also had the smallest standard error estimates, indicating high confidence in those effects. In all three species, adding climate normals made the interaction between interannual precipitation and temperature no longer significant.

3.1.1. *Douglas-fir*

30-year normal temperature significantly explained variation (across space) in growth, whereas 30-year normal precipitation did not (Fig. 4a). When climate normals were added, mean annual temperature became the largest, positive climate effect. The interaction between interannual and normal precipitation and the interaction between interannual temperature and normal precipitation was significant, indicating that there is spatial variation in the climate-sensitivity of Douglas-fir growth. The former was a negative effect, such that at higher average precipitation there is less of a positive effect of precipitation on growth (Fig. 4c), while the latter was a positive effect, such that at higher average precipitation there is less of a negative effect of temperature on growth (Fig. 4d). The interaction of SDI with both precipitation variables (interannual and normal) was significant. The interaction of SDI with interannual precipitation was positive, indicating that at high stand density there was a more positive effect of interannual precipitation on growth (Fig. 4e), while the interaction with normal precipitation was negative, indicating that at higher average precipitation there was a more negative effect of competition on growth (Fig. 4f).

3.1.2. *Ponderosa pine*

Precipitation and temperature normals did not themselves explain variation in ponderosa pine growth, but interactions between climate normals and other variables did significantly explain growth variation, including the interaction between interannual precipitation and both precipitation and temperature normals, as well as the interaction between BAL and 30-year normal precipitation (Fig. 5a). As with Douglas-fir, the interaction between interannual and normal precipitation was negative (Fig. 5c). The interaction between interannual precipitation and normal temperature was positive, indicating that at higher average temperature there is a more positive effect of precipitation on growth (Fig. 5d). The interaction between BAL and normal precipitation was negative, indicating that at high average precipitation there is a more negative effect of competition on growth (Fig. 5e).

3.1.3. *Engelmann spruce*

Climate normals alone did not significantly explain growth variability, but interactions between interannual precipitation and both climate normals (precipitation and temperature) were significant, as well as the interaction between interannual and normal temperature and between the competition variable BAL and interannual precipitation (Fig. 6a). As with ponderosa pine, the interaction between interannually varying precipitation and 30-year normal precipitation was negative (Fig. 6c), and the interaction between inter-annually varying precipitation and 30-year normal temperature was positive (Fig. 6d). The interaction between inter-annually varying temperature and 30-year normal temperature was negative, indicating that at higher average temperature there is a more negative effect of temperature on growth

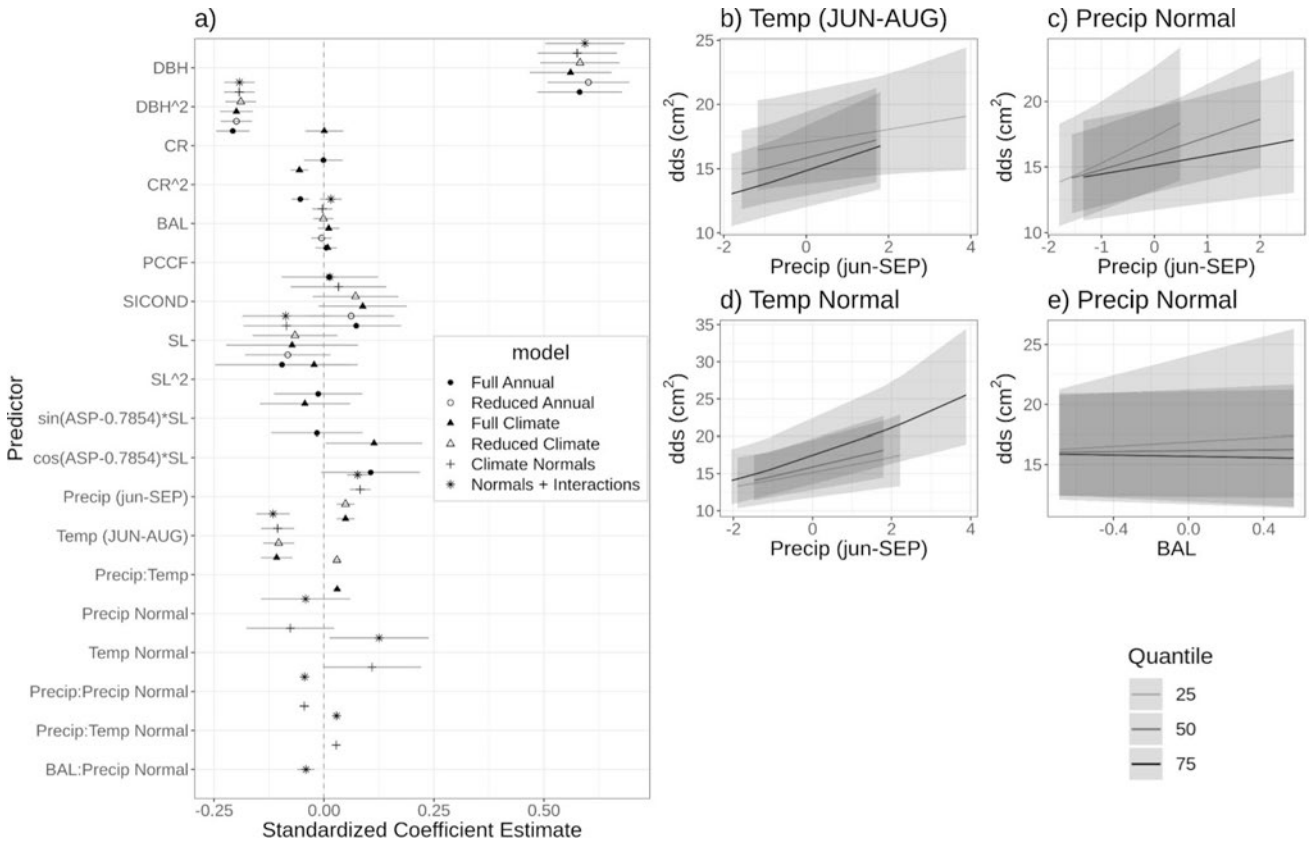

Fig. 5. Estimates of effects from ponderosa pine growth models. Standardized regression coefficients and their standard errors are shown in (a) for the predictors in all six models described in Fig. 2 and the text. Marginal effects of interaction terms on the growth response (dds) are shown, including the interaction between interannually varying precipitation (i.e., total precipitation [Precip] from previous June to current September [jun-SEP]) and interannually varying temperature (i.e., mean monthly max temperature [Temp] from current June to August [JUN-AUG]) (b), Precip (jun-SEP) and normal precipitation (Precip Normal) (c), Precip (jun-SEP) and normal temperature (Temp Normal) (d), and basal area of trees larger than the subject tree (BAL) and Precip Normal (e). Each of these panels shows one main effect (on the x-axis) conditional on the 25th, 50th, and 75th quantile of the other main effect (indicated in the panel title) with a 95% confidence interval around the prediction. Predicted effects are only plotted for known observations falling within the 95% confidence interval of the quantile.

(Fig. 6e). Finally, the interaction between BAL and interannual precipitation was positive, indicating that at higher levels of competition there is a more positive effect of precipitation on growth (Fig. 6f).

3.2. Validation

Across all species, the parameterization of growth models with tree-ring data improved performance compared to the baseline FVS large-tree diameter growth model with respect to the slope of the regression of observed vs. predicted diameter growth increment (Reduced Annual model, Fig. 7a). Across all metrics, the full models (Full Annual and Full Climate) did not perform better than the baseline FVS model, with the exception of the Full Climate model for ponderosa pine, which had a higher slope (Fig. 7a). For ponderosa pine and Engelmann spruce, all of the reduced models (Reduced Annual, Reduced Climate, Climate Normals, Normals + Interactions) outperformed the baseline FVS model in terms of slope (Fig. 7a). Model predictive performance was greatest with the Reduced Annual model for Douglas-fir, the Reduced Climate model for ponderosa pine, and both the Climate Normals and Normals + Interactions models for Engelmann spruce. For ponderosa pine, it was the baseline FVS model that had the lowest RMSE (0.5278) and highest R^2 (0.0728), compared to RMSE of 0.5305 and R^2 of 0.0633 of the Reduced Climate model, however, the match between predicted and observed diameter increment was greatly improved by the Reduced Climate model (slope of 0.5626 vs 0.1906). Overall, slope proved to be a better metric to compare alternative models, since it varied more widely within each species than the other two metrics of model performance. Although absolute values of RMSE and R^2 were low, values were consistent with out-of-sample validation, where only fixed effects are used in prediction (Supplementary Table 2).

Among the models parameterized with tree-ring data, the reduced models had higher performance than the full models across all three validation metrics. Adding climate predictors (both time-varying and normals) to Douglas-fir growth models lowered performance, in terms of slope, however, the Reduced Climate model performed indistinguishably well (i.e., high overlap in the confidence intervals) compared to the existing FVS growth model and the Reduced Annual model. In the case of ponderosa pine, adding climate normals to the Reduced Climate model lowered performance, whereas in the case of Engelmann spruce it improved performance.

Model performance at predicting out-of-sample data did not always align with calibration statistics (i.e., fit to calibration data). For example, while the addition of climate normals to interannually-varying climate predictors, along with their interactions, explained more of the variation in the calibration ring-width data, in terms of AIC (Supplemental Table 2), it did not consistently (i.e., across species) lead to increased performance at predicting out-of-sample diameter increments. In another example, for ponderosa pine, although SICOND and SL were found to be insignificant predictors of calibration data (Fig. 5a), model predictive performance improved with these terms included. Finally, in validation, for Douglas-fir, back-calculated CR outperformed constant CR as a metric of tree vigor, whereas for Engelmann spruce, constant CR outperformed back-calculated CR.

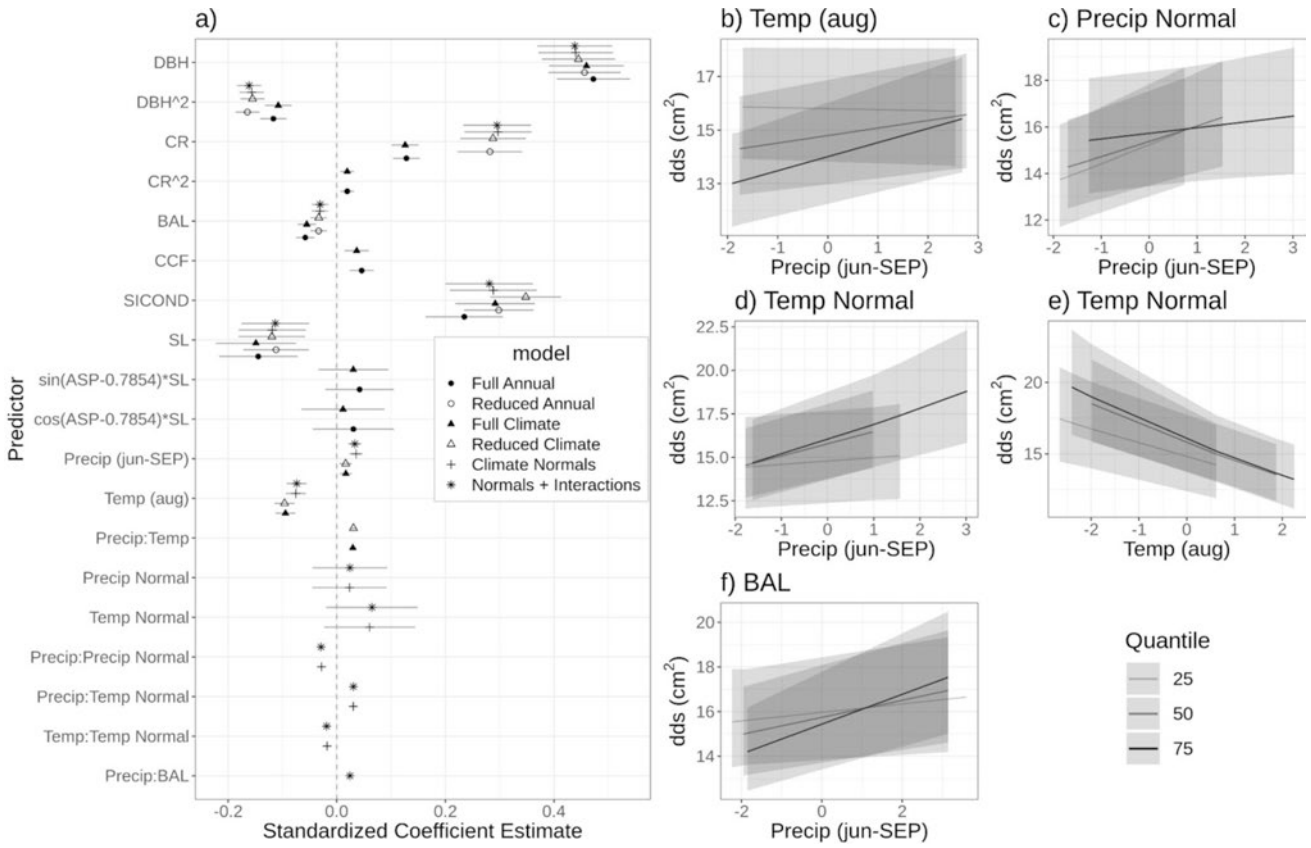

Fig. 6. Estimates of effects from Engelmann spruce growth models. Standardized regression coefficients and their standard errors are shown in (a) for the predictors in all six models described in Fig. 2 and the text. Marginal effects of interaction terms on the growth response (dds) are shown, including the interaction between interannually varying precipitation (i.e., total precipitation [Precip] from previous June to current September [jun-SEP]) and interannually varying temperature (i.e., monthly max temperature [Temp] from previous August [aug]) (b), Precip (jun-SEP) and normal precipitation (Precip Normal) (c), Precip (jun-SEP) and normal temperature (Temp Normal) (d), Temp (aug) and Temp Normal (e), and Precip (jun-SEP) and basal area of trees larger than the subject tree (f). Each of these panels shows one main effect (on the x-axis) conditional on the 25th, 50th, and 75th quantile of the other main effect (indicated in the panel title) with a 95% confidence interval around the prediction. Predicted effects are only plotted for known observations falling within the 95% confidence interval of the quantile.

3.3. Projection

Across all species, the Reduced Annual model predicted greater cumulative relative growth rate than the current FVS large-tree diameter growth model (Fig. 8a, c, and e). Further, the Reduced Annual model predicted greater cumulative relative growth rate than models with the effect of climate (i.e., Reduced Climate model, the Climate Normals model, and the Normals + Interactions model). There were species-specific differences for selected models with the effect of climate compared to the baseline FVS model. For Douglas-fir, these models all predicted more cumulative growth (Fig. 8a and b), but for ponderosa pine (Fig. 8c and d) and Engelmann spruce (Fig. 8e and f), these models predicted less cumulative growth than the baseline FVS model. For Engelmann spruce, we found that the Climate Normals and Normals + Interactions models had less of a reduction in cumulative growth from the baseline FVS model than the Reduced Climate model, but for Douglas-fir and ponderosa pine, the differences between these models were small. Across diameter classes, we found a greater difference in cumulative growth for lower diameter classes (Fig. 8b, d, and f). Finally, while the higher emission scenario, RCP8.5, on average predicted less growth than the lower emission scenario, RCP2.6, the difference was small.

4. Discussion

Returning to the research questions set forth for this work, we first asked what drives variation in tree growth. Integrating the annual-resolution information in tree-ring data with forest inventory data allowed us to quantify multiple drivers of tree growth acting simultaneously: interannual climate variability, competition, site index, and other factors (Fig. 4a, 5a and 6a). Notably, climate is a significant driver of growth variability. As expected across the arid state of Utah, all three study species are positively sensitive to precipitation variability and negatively sensitive to temperature variability. While the estimated magnitude of climate effects is small (as are the effects of competition variables; Fig. 4a, 5a and 6a), they are well constrained, and they will compound over time by impacting growth year after year.

A second question then was whether the addition of climate effects in FVS's large tree diameter growth model improves prediction. Models parameterized with tree-ring data and simplified by removing terms (i.e., reduced models) consistently outperformed the Utah variant's current large tree diameter growth model at predicting out-of-sample growth increments, suggesting that the existing model is overly complex. Beyond this, which model performed best differed between species (Fig. 7). Performance of the current FVS diameter growth model for Douglas-fir is already high, in terms of bias (Fig. 7a), such that adding climate effects did not improve prediction, at least not over the short time span of ten years. In contrast, for ponderosa pine and Engelmann spruce, the current FVS growth model is biased towards predicting larger growth increments than are observed, and the addition of climate effects reduced this bias (Fig. 7a), even over the short time span of ten years. One possible interpretation is that ponderosa pine and Engelmann spruce, which are found in low- and high-elevation forests in Utah, respectively, are more climate-limited or more exposed to the effects of

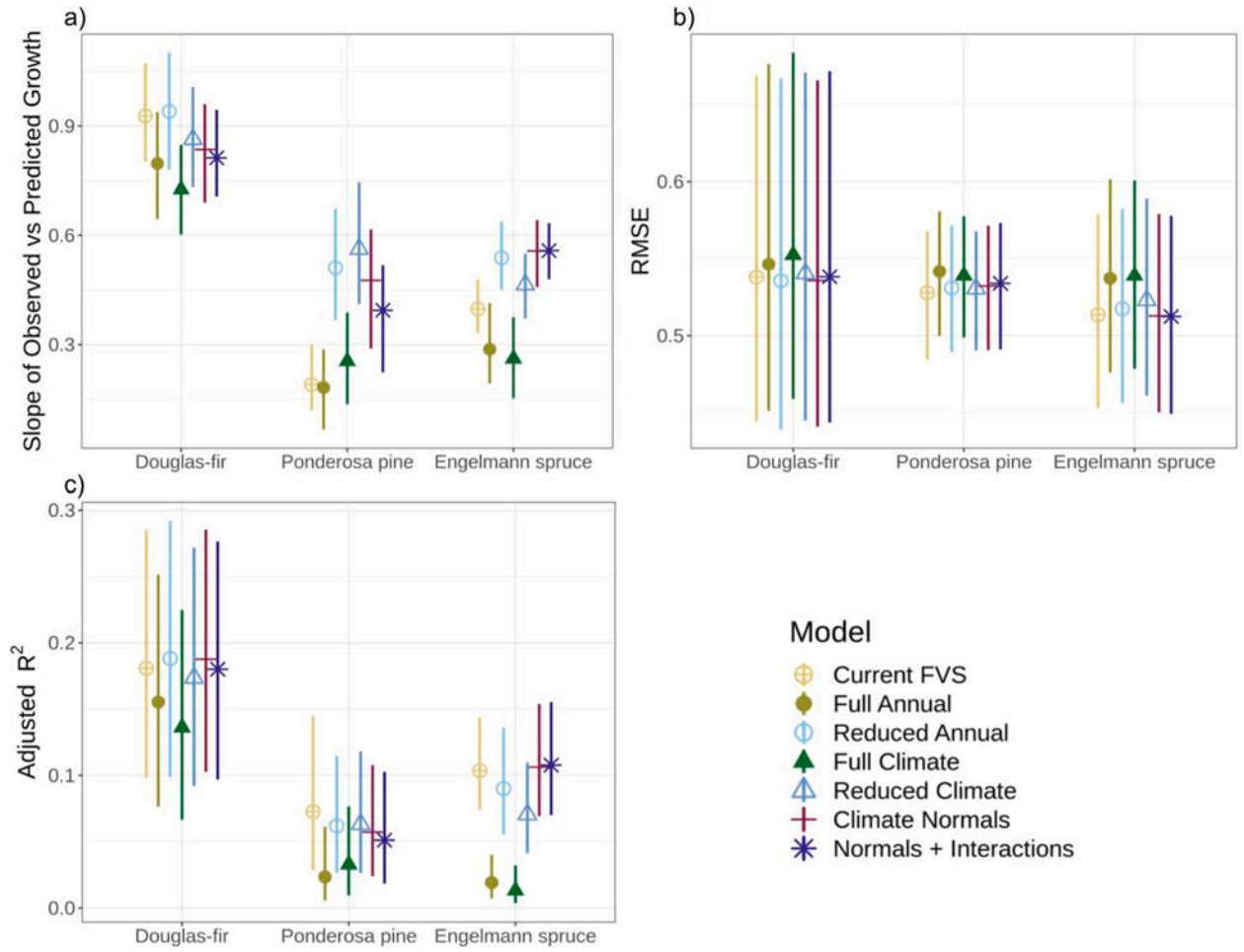

Fig. 7. Validation of six alternative diameter growth models (described in Fig. 2 and the text) for Douglas-fir, ponderosa pine, and Engelmann spruce. Model performance is assessed in terms of adjusted R^2, root mean square error (RMSE), and the slope of the linear regression of observed vs. predicted diameter growth increment. Confidence intervals for adjusted R^2 and RMSE were derived from bootstrapping.

climate change, whereas Douglas-fir, positioned at neither elevation extreme, is less climate-limited or less exposed to changing climate. For a well-calibrated species like Douglas-fir, it may be that the addition of climate effects would improve prediction over a longer time frame, but this remains to be demonstrated. Model validation thus suggests that for species with low performance in FVS, parameterization with tree rings improves prediction of growth, and thus that a tree ring-based, climate-sensitive version of FVS should make more realistic estimates of the carbon uptake potential of trees experiencing climate change.

Our third question concerned what future growth of the study species might look like, based upon improved models of growth. Projecting forward in time with the effect of climate change explicitly accounted for, we can expect reduced growth of ponderosa pine and Engelmann spruce, compared to what is predicted by the current FVS model (Fig. 8c-f). In contrast, projection results suggest we might expect more growth for Douglas-fir than what is currently predicted by FVS (Fig. 8a and b). However, we caution against the interpretation that Douglas-fir in Utah will be resilient in the face of changing climate. For all species, adding the effect of climate to a tree-ring parameterized model reduced predicted growth (i.e., the Reduced Annual model vs. the Reduced Climate model; Fig. 8a, c, and e). We suggest a sensitivity analysis be performed to identify the variables most strongly influencing predicted growth. Together, these results argue for the incorporation of climate effects into FVS, to better anticipate forest climate mitigation potential, and demonstrate the feasibility of doing so directly, using tree-ring data. In the following, we consider additional insights into tree growth offered by our analyses, and what further improvements we anticipate can be made to the large tree diameter growth model.

4.1. *Refined understanding of the drivers of tree growth variability*

Tree growth is influenced by several factors at once; here, we consider insights into these effects, starting with climate effects, and how they interact with other drivers, followed by the effects of competition proxies. Positive precipitation sensitivity and negative temperature sensitivity of the growth of all three study species is consistent with widespread moisture-limited tree growth across the interior western U.S. (Chen et al., 2010; Rinaldi et al., 2021). Unlike spruce in some parts of the boreal zone, where growth can be temperature-limited, high-elevation spruce in the western U.S. exhibits both (positive) precipitation and (negative) temperature signal (Buechling et al., 2017). Indeed, even at high latitudes, growth of Engelmann spruce can have a strong negative relationship with previous growing season temperature (Hart and Laroque, 2013).

Beyond negative sensitivity to temperature and positive sensitivity to precipitation, tree-ring data allowed us to detect spatial variation in the sensitivity of tree growth to time-varying climate. We found stronger climate sensitivities (steeper slope of the response to time-varying climate) at dry and warm locations (Fig. 4c and d, Fig. 5c and d, and Fig. 6c-e), confirming the hypothesis articulated by Fritts et al. (1965) that spatial variation in climate sensitivity is governed by average climate conditions. Our interpretation is that tree growth is limited by soil moisture across all three of the study species and that climate sensitivity increases as soil moisture becomes more limiting. Tree-ring

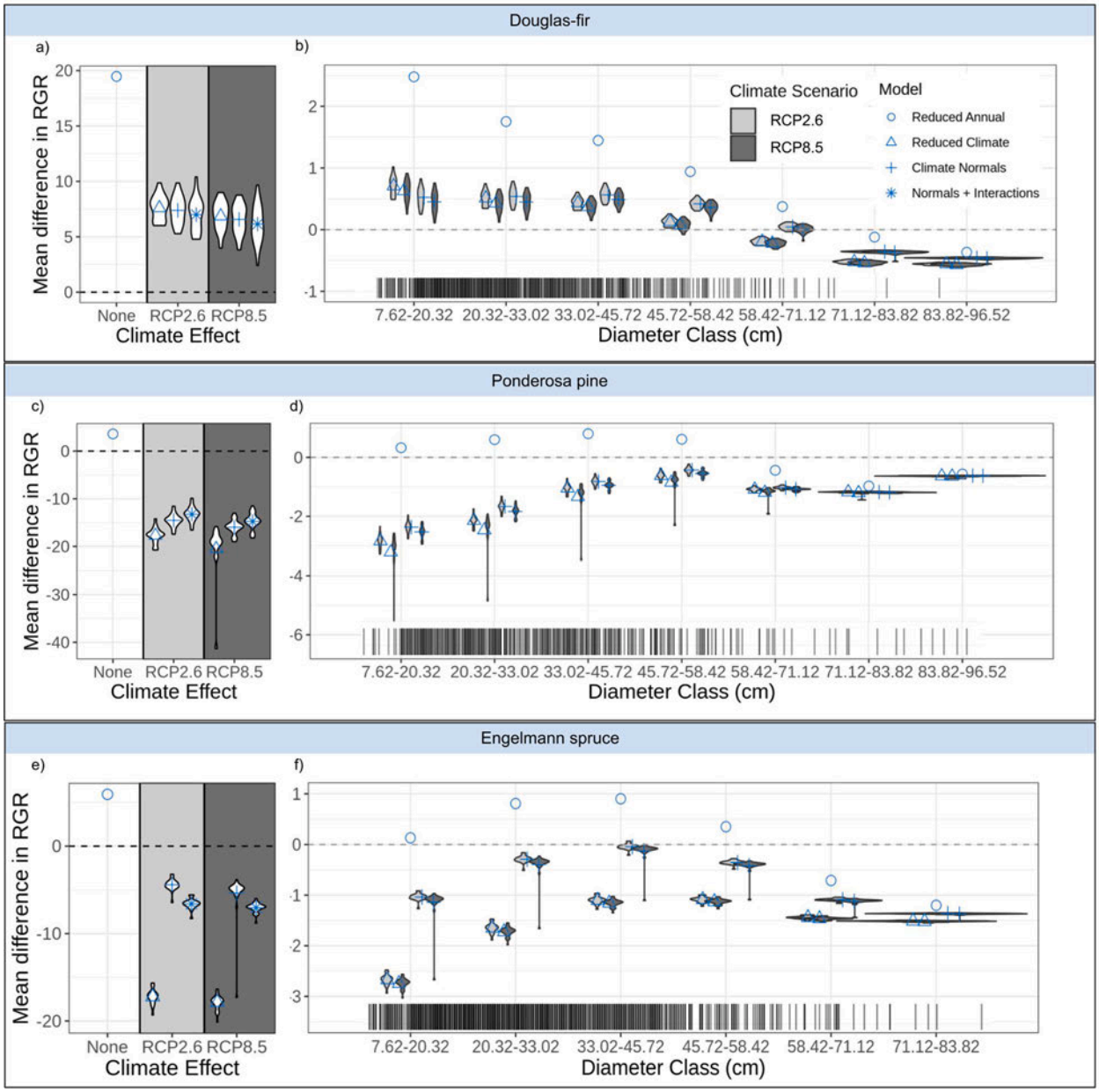

Fig. 8. Difference in projected growth, for Douglas-fir (a-b), ponderosa pine (c-d), and Engelmann spruce (e-f), between high-performing updated models and the Forest Vegetation Simulator (FVS). Average difference in cumulative relative growth rate (RGR) projected for all trees (a,c,e) and for seven 5-inch diameter classes from 3 to 38 in. (b,d,f), comparing projections from FVS vs. a model with no climate effects (i.e., Reduced Annual) or climate effects given future scenarios of RCP2.6 or RCP8.5 (i.e., Reduced Climate, Climate Normal, or Normals + Interactions). Negative values indicate a tree-ring-informed model predicted less growth than the current FVS model, whereas positive values indicate a tree-ring-informed model predicted more growth than FVS. Variation among general circulation model climate projections (Supplementary Table 1) is indicated by the distribution around the mean and the rug shows the distribution of tree size at the start of the projection time period.

data make it possible to capture heterogeneity in climate response beyond the location adjustment provided by the current FVS growth model and at higher temporal resolution than Climate-FVS. This heterogeneity seems to be particularly important in Engelmann spruce, since projected reductions in growth caused by negative temperature sensitivity were less extreme when spatial variation in climate sensitivity was explicitly accounted for (the Climate Normals and Normals + Interactions models in Fig. 8c). For a high-elevation species, accounting for heterogeneity in growth-limiting factors may be critical to identify areas of greater vs. lesser vulnerability to climate change.

By incorporating the effect of climate on growth directly in a multiple regression model, rather than through the climate envelope approach of Climate-FVS, we were able to explicitly model interactions between climate and tree- or stand-level characteristics. These interactions are particularly important because managers cannot manipulate climate, but they can influence some of the other drivers of tree growth that may interact with climate. For example, consistent with other analyses addressing the effects of both climate and competition on tree growth (Buechling et al., 2017), we found that competition alters the response of growth to climate variability. Increased competition within a stand increases climate sensitivities (Fig. 4e and Fig. 6f), suggesting that forests can be managed to mitigate the impact of climate variability and change by reducing stand density. In addition, we found climate-driven spatial variation in the response to competition: trees in a drier region of their climatic range are less negatively impacted by the presence of other trees (Fig. 4f and Fig. 5e). The benefit of more or larger

neighbors at these sites may reflect facilitation through microclimate effects, but further exploration with more data, or ideally through experimentation, is needed to verify these effects.

In addition to climate effects and interaction effects involving climate, parameterization with tree rings allowed us to critically examine which among several competition variables best captured negative density-dependent regulation. These competition variables are designed to capture different competitive mechanisms. One-sided (asymmetric) competition variables, such as BAL, consider competition only from trees larger than the subject tree, with competition for light in mind, whereas two-sided (symmetric) competition parameters, such as CCF, PCCF, and SDI, consider competition from both sides of the diameter distribution relative to the subject tree, with competition for below-ground resources in mind, such as soil moisture and nutrients (Weiskittel et al., 2011). To capture both of these mechanisms, both categories of competition variables are often included in models of tree growth (Weiskittel et al., 2011). However, which type of competition variable best explains growth may depend on the ecology of the species (Pretzsch and Biber, 2010). Canham et al. (2004) experimentally separated the effect of aboveground and belowground competition and found that shade tolerant trees were more sensitive to crowding (two-sided) rather than shading (one-sided), supporting the idea that one-sided competition variables capture competition for light. But in our case, the competition predictors retained across species did not match cross-species patterns of shade tolerance. Growth in both the least shade-tolerant species, ponderosa pine, and the most shade-tolerant, Engelmann spruce, was best explained by a one-sided competition variable, BAL. How best to represent competition in individual-tree growth and yield models remains a worthy area of investigation, as the process should be expected to vary, in mechanism and magnitude, across species limited by different resources or along environmental gradients.

4.2. Opportunities for future improvement

Our work suggests several avenues for further improvement of a climate-sensitive growth model in the FVS. Inference from empirical models depends directly on the quantity and quality of the data used in calibration. For example, the statistically insignificant effects in the ponderosa pine growth model (Fig. 5a) may reflect the limited available sample size (n = 69 increment cores). Further, better data on the predictors in the growth model should better constrain their effects. Shortcomings in the predictors might include 1) not fully capturing the range of values of a driver during calibration, leading to extrapolation of effects, e.g., temperature that exceeds the historical range of variability, and 2) imperfect estimation of unobserved drivers, i.e., through proxies or observable metrics. In the following, we consider these issues for several predictors of growth: climate, then tree size (DBH), then competition, and finally site quality (SICOND).

Tree rings offer a way to empirically estimate the climate sensitivity of growth for many species, but projection of future growth relies on tree responses to future climate being the same as their responses to past climate, an assumption known in dendrochronology as "uniformitarianism" (Fritts, 1976). Violating this assumption, tree growth responses to climate variability are shifting with changing climate in the latter part of the 20th and early 21st centuries, e.g., from positive to negative sensitivity to temperature variability at high latitudes (Babst et al., 2019). The general principle, that a model may fit well to calibration data but extrapolate poorly to novel conditions, is particularly relevant in a global change context (Evans, 2012). To try to capture how the climate sensitivity of tree growth might change with, for example, increasingly warmer average temperature, we included an interaction between average and interannual climate predictors. However, this approach relies on space-for-time substitution (Pickett, 1989), which assumes that the past response of a tree at a warmer (on average) location can be projected (substituted) for a tree at a currently cooler location when it experiences a warmer future. This assumption is problematic because it presumes that locally adapted genotypes can be treated as substitutable, or that the process of local adaptation is instantaneous (Klesse et al., 2020). For this reason, we did not apply future climate data to climate normals during projection of future growth, following the example of Klesse et al. (2020). Future climate data were used for time-varying temperature and precipitation variables, so that we captured how climate sensitivities might change with non-stationary climate (*sensu* Klesse et al., 2020).

Two other approaches that might be used in the future, in terms of addressing the problem of extrapolation of climate sensitivities, are first, to estimate a nonlinear climate response, i.e., increased climate sensitivity as temperature increases. Nonlinear responses can be modeled with a quadratic term on the time-varying climate predictors, or by using a GAM, spline, or other basis function. A second, slightly less statistical approach is to incorporate outputs from a physiological model driven by climate. Milner et al. (2003) linked the physiological model STAND-BGC to FVS, though their estimates of the relationship between climate and growth did not account for local adaptation (Crookston et al., 2005). Tree-ring data can be used to fit a model that is based on a more physiological understanding of tree growth (the Vaganov-Shashkin model; Mina et al.,2016; Tolwinski-Ward et al., 2011), and doing so with locally-sourced data would account for local adaptation with respect to non-linear or threshold-like responses of tree growth to increasingly warm temperatures.

Consistent with other individual tree growth models (Monserud and Sterba, 1996), we found tree-level predictors, DBH and CR, to have the largest effect on diameter growth. Because of the magnitude of these effects, it is particularly important for calibration data to span the full range of these predictors. However, we had relatively little data on very large trees for calibration of the growth model (Supplementary Fig. 7); this skewed sample distribution can lead to bias in estimated growth rates (Bowman et al., 2013). Further, we note that the greatest contrast in predicted growth between our models vs. the current FVS model falls at the small tree size-class (Fig. 8b, d, and f). We suggest that data collection efforts should focus on broadening the diameter distribution by increasing the sample size of trees that are cored to include more small or young trees and large or old trees, so that size-related growth responses can be better constrained.

A persistent challenge in forest models is historical information on competitive conditions - the number and size of trees in the stand. Without repeated measurement of trees spanning decades, the competitive environment must be back-calculated. This leads to error or uncertainty in competition variables, which will inevitably increasingly diverge from the true, but unknown past forest stand structure (Swetnam et al., 1999). Tree rings offer a way to directly calculate attributes from tree- to stand-level for annual growth models, even with repeated measurements, in contrast to the methods used by Cao (2000) and Weiskittel (2007). However, for the competitive environment to be annualized using tree rings, increments are needed for every tree on the plot. To improve upon the method used here and other methods for back-calculation of annual stand density (Cao and Strub, 2008), we suggest the collection of increment cores from all trees per plot, in a focused study, to more precisely calculate annual competition predictors.

We treated the site-level biophysical variable SICOND as constant through time. However, site index is a purely phenomenological measure of site quality that depends on site-level properties, including soil properties and microclimate (Monserud et al., 2008), and can therefore be expected to change with climate (as well as disturbances). In Climate-FVS, site index change is modified proportionally with climate suitability, which can modify expected growth (Crookston et al., 2010). An alternative would be to explicitly model the factors that determine the height vs. age relationship quantified by site index, including the direct effect of climate on height growth rate. Starting with these opportunities for improvement, a re-engineering of the large-tree diameter growth model, already invoked by Pokharel and Froese (2008), could better

capture the processes influencing tree growth in a changing climate.

5. Conclusion

This work demonstrates that the addition of tree-ring data to the forest inventory data normally used in parameterizing the FVS large-tree diameter growth model makes it possible to explicitly account for an important driver of tree growth (climate) and increase predictive performance. Changing climate will modify the growth rate of trees, potentially altering the rate at which carbon storage potential is achieved (Giebink et al., 2022) or the carbon carrying capacity of a forest stand, i.e., maximum SDI (Kubiske et al., 2019). Thus this update addresses an important need in forest management in the U. S. - for a tree growth model with the direct effect of interannual climate variability. The workflow we have developed for three species under the Utah variant of FVS, which is hosted on a publicly available repository (https://github.com/clgiebink/UT_FVS), can be used along with a tree-ring data network sourced in forest inventory plots (DeRose et al., 2017; Evans et al., 2021) to make locally parameterized climate-sensitive diameter growth models for other species and in other variants of FVS across the U.S. The next step is to incorporate climate-sensitive diameter growth models into FVS, which is a widely used decision support tool and carbon market-approved forest carbon calculator (California Air Resources Board, 2015). By incorporating the direct effect of climate into a stand-level management tool, targeted management, e.g., thinning of specific size classes, can be explored as a means to reduce these vulnerabilities associated with changing climate. Indeed, forest managers are increasingly called upon to estimate the carbon consequences of management decisions, and stand-level models are well-suited to do so (Moore et al., 2012; Puhlick et al., 2020; Zald et al., 2016). An annualized, climate-sensitive version of FVS, paired with an annualized inventory, would support near-term iterative forecasting and adaptive management by foresters (Dietze et al., 2018; Walters, 1986). That is, after a management decision is put into action based on a projection of forest vulnerability, incoming forest inventory measurements would provide observations from which to validate model projections as well as modify and improve the forest simulator. This sort of locally parameterized and climate-sensitive FVS would allow foresters to better characterize and plan for climate vulnerability and expected climate impacts specific to their management unit.

CRediT authorship contribution statement

Courtney L. Giebink: Methodology, Software, Formal analysis, Writing – original draft, Writing – review & editing, Visualization. **R. Justin DeRose:** Conceptualization, Writing – review & editing, Investigation, Data curation. **Mark Castle:** Software, Writing – review & editing. **John D. Shaw:** Conceptualization, Writing – review & editing, Resources. **Margaret E.K. Evans:** Methodology, Conceptualization, Writing – review & editing, Supervision.

Declaration of Competing Interest

The authors declare that they have no known competing financial interests or personal relationships that could have appeared to influence the work reported in this paper.

Acknowledgements

We acknowledge the World Climate Research Programme's Working Group on Coupled Modelling, which is responsible for CMIP, and we thank the climate modeling groups (listed in Supplementary Table 1) for producing and making available their model output. For CMIP, the U.S. Department of Energy's Program for Climate Model Diagnosis and Intercomparison provides coordinating support and led development of software infrastructure in partnership with the Global Organization for Earth System Science Portals. Finally, we thank code contributions from Jeff Oliver, Kelly Heilman, and Michiel Pillet.

Funding

This research was supported [in part] by the U.S. Department of Agriculture, Forest Service. MEKE was supported by NSF Macrosystems ECA 1802893. RJD was supported by the Utah Agricultural Experiment Station, Utah State University, and approved as journal paper number 9550.

Appendix A. Supplementary data

Supplementary data to this article can be found online at https://doi.org/10.1016/j.foreco.2022.120256.

References

Aitken, S.N., Bemmels, J.B., 2016. Time to get moving: assisted gene flow of forest trees. Evol. Appl. 9 (1), 271–290.
Akaike, H., 1974. A new look at the statistical model identification. IEEE Trans. Automat. Contr. 19 (6), 716–723.
Alberto, F.J., Aitken, S.N., Alía, R., González-Martínez, S.C., Hänninen, H., Kremer, A., Lefèvre, F., Lenormand, T., Yeaman, S., Whetten, R., Savolainen, O., 2013. Potential for evolutionary responses to climate change - evidence from tree populations. Glob. Chang. Biol. 19 (6), 1645–1661.
Albrich, K., Rammer, W., Turner, M.G., Ratajczak, Z., Braziunas, K.H., Hansen, W.D., Seidl, R., Hickler, T., 2020. Simulating forest resilience: A review. Glob. Ecol. Biogeogr. 29 (12), 2082–2096.
Arner, S.L., Woudenberg, S., Waters, S., Vissage, J., Maclean, C., Thompson, M., Hansen, M., 2001. National Algorithms for Determining Stocking Class, Stand Size Class, and Forest Type for Forest Inventory and Analysis Plots.
Babst, F., Bouriaud, O., Poulter, B., Trouet, V., Girardin, M.P., Frank, D.C., 2019. Twentieth century redistribution in climatic drivers of global tree growth. Sci. Adv. 5 https://doi.org/10.1126/sciadv.aat4313.
Bates, D., Mächler, M., Bolker, B., Walker, S., 2015. Fitting Linear Mixed-Effects Models Using lme4. J. Stat. Softw. 67. https://doi.org/10.18637/jss.v067.i01.
Bohner, T., Diez, J., Coulson, T., 2020. Extensive mismatches between species distributions and performance and their relationship to functional traits. Ecol. Lett. 23 (1), 33–44. https://doi.org/10.1111/ele.13396.
Bowman, D.M.J.S., Brienen, R.J.W., Gloor, E., Phillips, O.L., Prior, L.D., 2013. Detecting trends in tree growth: Not so simple. Trends Plant Sci 18 (1), 11–17. https://doi.org/10.1016/j.tplants.2012.08.005.
Buechling, A., Martin, P.H., Canham, C.D., Piper, F., 2017. Climate and competition effects on tree growth in Rocky Mountain forests. J. Ecol. 105 (6), 1636–1647. https://doi.org/10.1111/1365-2745.12782.
Bugmann, H., 2001. A review of forest gap models. Clim. Change. https://doi.org/10.1023/A:1012525626267.
Bunn, A.G., 2008. A dendrochronology program library in R (dplR). Dendrochronologia 26 (2), 115–124.
Burrill, E.A., Wilson, A.M., Turner, J.A., Pugh, S.A., Menlove, Christensen, Conkling, B. L., David, 2018. The Forest Inventory and Analysis Database: Database Description and User Guide for Phase 2 (version 8.0). Available at: https://www.fia.fs.fed.us/library/database-documentation/current/ver80/FIADB%20User%20Guide%20P2_8-0.pdf.
California Air Resources Board, 2015. Compliance Offset Protocol U.S. Forest Projects. Available at https://ww2.arb.ca.gov/sites/default/files/cap-and-trade/protocols/usforest/forestprotocol2015.pdf.
Canham, C.D., LePage, P.T., Coates, K.D., 2004. A neighborhood analysis of canopy tree competition: effects of shading versus crowding. Can. J. For. Res. 34 (4), 778–787.
Canham, C.D., Murphy, L., Riemann, R., McCullough, R., Burrill, E., 2018. Local differentiation in tree growth responses to climate. Ecosphere 9, 1–12. https://doi.org/10.1002/ecs2.2368.
Cao, Q., Strub, M., 2008. Evaluation of Four Methods to Estimate Parameters of an Annual Tree Survival and Diameter Growth Model. For. Sci. 54, 617–624.
Cao, Q.V., 2000. Prediction of Annual Diameter Growth and Survival for Individual Trees from Periodic Measurements. For. Sci. 46, 127–131.
Cawrse, D., Keyser, C., Keyser, T., Sanchez Meador, A., Smith-Mateja, E., Van Dyck, M., 2010. Forest Vegetation Simulator Model Validation Protocols. Fort Collins, CO. Available at https://www.fs.fed.us/fmsc/ftp/fvs/docs/steering/FVS_Model_Validation_Protocols.pdf.
Chen, P.-Y., Welsh, C., Hamann, A., 2010. Geographic variation in growth response of Douglas-fir to interannual climate variability and projected climate change. Glob. Chang. Biol. 16, 3374–3385. https://doi.org/10.1111/j.1365-2486.2010.02166.x.
Crookston, N.L., Dixon, G.E., 2005. The forest vegetation simulator: A review of its structure, content, and applications. Comput. Electron. Agric. 49, 60–80. https://doi.org/10.1016/j.compag.2005.02.003.
Crookston, N.L., Rehfeldt, G.E., Dixon, G.E., Weiskittel, A.R., 2010. Addressing climate change in the forest vegetation simulator to assess impacts on landscape forest dynamics. For. Ecol. Manage. 260, 1198–1211. https://doi.org/10.1016/j.foreco.2010.07.013.

Crookston, N.L., Rehfeldt, G.E., Warwell, M.V, 2005. Using Forest Inventory and Analysis Data To Model Plant-Climate Relationships. In: McRoberts, R.E., Reams, G.A., Van Deusen, P.C., McWilliams, W.H. (eds.), Proceedings of the Seventh Annual Forest Inventory and Analysis Symposium, volume 23, pp. 243–250. U.S. Department of Agriculture Forest Service, Portland, ME.

Daly, C., Halbleib, M., Smith, J.I., Gibson, W.P., Doggett, M.K., Taylor, G.H., Curtis, J., Pasteris, P.P., 2008. Physiographically sensitive mapping of climatological temperature and precipitation across the conterminous United States. Int. J. Climatol. 28, 2031–2064. https://doi.org/10.1002/joc.1688.

DeRose, R.J., Shaw, J.D., Long, J.N., 2017. Building the forest inventory and analysis tree-ring data set. J. For. 115, 283–291. https://doi.org/10.5849/jof.15-097.

DeRose, R.J., Shaw, J.D., Long, J.N., 2011. Validation of the Utah and Western Sierra Variants of the Forest Vegetation Simulator. Available at. http://works.bepress.com/justin-derose/45/.

DeRose, R.J., Wang, S.Y., Shaw, J.D., 2013. Feasibility of high-density climate reconstruction based on forest inventory and analysis (FIA) collected tree-ring data. J. Hydrometeorol. 14, 375–381. https://doi.org/10.1175/JHM-D-12-0124.1.

Dietze, M.C., Fox, A., Beck-Johnson, L.M., Betancourt, J.L., Hooten, M.B., Jarnevich, C.S., Keitt, T.H., Kenney, M.A., Laney, C.M., Larsen, L.G., Loescher, H.W., Lunch, C.K., Pijanowski, B.C., Randerson, J.T., Read, E.K., Tredennick, A.T., Vargas, R., Weathers, K.C., White, E.P., 2018. Iterative near-term ecological forecasting: Needs, opportunities, and challenges. Proc. Natl. Acad. Sci. 115, 1424–1432. https://doi.org/10.1073/pnas.1710231115.

Dixon, G.E., 2002. Essential FVS: A User's Guide to the Forest Vegetation Simulator. USDA Forest Service, Forest Management Service Center, Fort Collins, CO. Available at https://www.fs.fed.us/.ftproot/pub/fmsc/ftp/fvs/docs/gtr/EssentialFVS.pdf.

Dixon, G.E., 1985. Crown ratio modeling using stand density index and the Weibull distribution. Lutsen, Minnesota.

Dormann, C.F., Elith, J., Bacher, S., Buchmann, C., Carl, G., Carré, G., Marquéz, J.R.G., Gruber, B., Lafourcade, B., Leitão, P.J., Münkemüller, T., McClean, C., Osborne, P.E., Reineking, B., Schröder, B., Skidmore, A.K., Zurell, D., Lautenbach, S., 2013. Collinearity: a review of methods to deal with it and a simulation study evaluating their performance. Ecography (Cop.) 36 (1), 27–46. https://doi.org/10.1111/j.1600-0587.2012.07348.x.

Evans, M.R., 2012. Modelling ecological systems in a changing world. Philos. Trans. R. Soc. B Biol. Sci. 367, 181–190. https://doi.org/10.1098/rstb.2011.0172.

Evans, M.E.K., DeRose, R.J., Klesse, S., Girardin, M.P., Heilman, K.A., Alexander, M.R., Arsenault, A., Babst, F., Bouchard, M., Cahoon, S.M.P., Campbell, E.M., Dietze, M., Duchesne, L., Frank, D.C., Giebink, C.L., Gómez-Guerrero, A., García, G.G., Hogg, E. H., Metsaranta, J., Ols, C., Rayback, S.A., Reid, A., Ricker, M., Schaberg, P.G., Shaw, J.D., Sullivan, P.F., Gaytán, S.A.V., 2021. Adding tree rings to North America's national forest inventories: An essential tool to guide drawdown of atmospheric CO_2. Bioscience. https://doi.org/10.1093/biosci/biab119.

Fargione, J.E., Bassett, S., Boucher, T., Bridgham, S.D., Conant, R.T., Cook-Patton, S.C., Ellis, P.W., Falcucci, A., Fourqurean, J.W., Gopalakrishna, T., Gu, H., Henderson, B., Hurteau, M.D., Kroeger, K.D., Kroeger, T., Lark, T.J., Leavitt, S.M., Lomax, G., Mcdonald, R.I., Megonigal, J.P., Miteva, D.A., Richardson, C.J., Sanderman, J., Shoch, D., Spawn, S.A., Veldman, J.W., Williams, C.A., Woodbury, P.B., Zganjar, C., Baranski, M., Elias, P., Houghton, R.A., Landis, E., Mcglynn, E., Schlesinger, W.H., Siikamaki, J.V., Sutton-Grier, A.E., Griscom, B.W., 2018. Natural climate solutions for the United States. Sci. Adv 4. https://doi.org/10.1126/sciadv.aat1869.

Fisher, R.A., Koven, C.D., Anderegg, W.R.L., Christoffersen, B.O., Dietze, M.C., Farrior, C. E., Holm, J.A., Hurtt, G.C., Knox, R.G., Lawrence, P.J., Lichstein, J.W., Longo, M., Matheny, A.M., Medvigy, D., Muller-Landau, H.C., Powell, T.L., Serbin, S.P., Sato, H., Shuman, J.K., Smith, B., Trugman, A.T., Viskari, T., Verbeeck, H., Weng, E., Xu, C., Xu, X., Zhang, T., Moorcroft, P.R., 2018. Vegetation demographics in Earth System Models: A review of progress and priorities. Glob. Chang. Biol. 24 (1), 35–54. https://doi.org/10.1111/gcb.13910.

Foley, J.A., Prentice, I.C., Ramankutty, N., Levis, S., Pollard, D., Sitch, S., Haxeltine, A., 1996. An integrated biosphere model of land surface processes, terrestrial carbon balance, and vegetation dynamics. Global Biogeochem. Cycles 10, 603–628. https://doi.org/10.1029/96GB02692.

Forest Inventory and Analysis Database, St. Paul, MN: U.S. Department of Agriculture, Forest Service, Northern Research Station. 2022. Available: https://apps.fs.usda.gov/fia/datamart/CSV/datamart_csv.html.

Fox, J., Weisberg, S., 2019. An R Companion to Applied Regression, Third. ed. Sage, Thousand Oaks, CA.

Fritts, H., 1976. Tree rings and climate. Academic Press, London, UK.

Fritts, H.C., Smith, D.G., Cardis, J.W., Budelsky, C.A., 1965. Tree-Ring Characteristics Along a Vegetation Gradient in Northern Arizona. Ecology 46 (4), 393–401.

Giebink, C., 2022. UT_rw. CyVerse Data Commons. https://doi.org/10.25739/vtef-zg41.

Giebink, C.L., Domke, G.M., Fisher, R.A., Heilman, K.A., Moore, D.J.P., DeRose, R.J., Evans, M.E.K., 2022. The policy and ecology of forest-based climate mitigation: challenges, needs and opportunities. Plant Soil. https://doi.org/10.1007/s11104-022-05315-6.

Grassi, G., House, J., Dentener, F., Federici, S., Den Elzen, M., Penman, J., 2017. The key role of forests in meeting climate targets requires science for credible mitigation. Nat. Clim. Chang. 7, 220–226. https://doi.org/10.1038/nclimate3227.

Griscom, B.W., Adams, J., Ellis, P.W., Houghton, R.A., Lomax, G., Miteva, D.A., Schlesinger, W.H., Shoch, D., Siikamäki, J.V., Smith, P., Woodbury, P., Zganjar, C., Blackman, A., Campari, J., Conant, R.T., Delgado, C., Elias, P., Gopalakrishna, T., Hamsik, M.R., Herrero, M., Kiesecker, J., Landis, E., Laestadius, L., Leavitt, S.M., Minnemeyer, S., Polasky, S., Potapov, P., Putz, F.E., Sanderman, J., Silvius, M., Wollenberg, E., Fargione, J., 2017. Natural climate solutions. Proc. Natl. Acad. Sci. U. S. A. 114, 11645–11650. https://doi.org/10.1073/pnas.1710465114.

Hart, S.J., Laroque, C.P., 2013. Searching for thresholds in climate–radial growth relationships of Engelmann spruce and subalpine fir, Jasper National Park, Alberta, Canada. Dendrochronologia 31, 9–15. https://doi.org/10.1016/j.dendro.2012.04.005.

Housset, J.M., Nadeau, S., Isabel, N., Depardieu, C., Duchesne, I., Lenz, P., Girardin, M. P., 2018. Tree rings provide a new class of phenotypes for genetic associations that foster insights into adaptation of conifers to climate change. New Phytol. 218, 630–645. https://doi.org/10.1111/nph.14968.

Keyser, C.E., Dixon, G.E., 2019. Utah (UT) Variant Overview - Forest Vegetation Simulator. Fort Collins, CO.

Klesse, S., DeRose, R.J., Babst, F., Black, B.A., Anderegg, L.D.L., Axelson, J., Ettinger, A., Griesbauer, H., Guiterman, C.H., Harley, G., Harvey, J.E., Lo, Y.H., Lynch, A.M., O'Connor, C., Restaino, C., Sauchyn, D., Shaw, J.D., Smith, D.J., Wood, L., Villanueva-Díaz, J., Evans, M.E.K., 2020. Continental-scale tree-ring-based projection of Douglas-fir growth: Testing the limits of space-for-time substitution. Glob. Chang. Biol. 26, 5146–5163. https://doi.org/10.1111/gcb.15170.

Klesse, S., DeRose, R.J., Guiterman, C.H., Lynch, A.M., O'Connor, C.D., Shaw, J.D., Evans, M.E.K., 2018. Sampling bias overestimates climate change impacts on forest growth in the southwestern United States. Nat. Commun. 9, 5336. https://doi.org/10.1038/s41467-018-07800-y.

Krajicek, J.E., Brinkman, K.A., Gingrich, S.F., 1961. Crown competition - A measure of density. For. Sci. 7, 35–42.

Kubiske, M.E., Woodall, C.W., Kern, C.C., 2019. Increasing atmospheric CO2 concentration stand development in trembling aspen forests: Are outdated density management guidelines in need of revision for all species? J. For. 117, 38–45. https://doi.org/10.1093/jofore/fvy058.

Kuznetsova, A., Brockhoff, P.B., Christensen, R.H.B., 2017. lmerTest Package: Tests in Linear Mixed Effects Models. J. Stat. Softw. 82. https://doi.org/10.18637/jss.v082.i13.

Langlet, O., 1971. Two hundred years genecology. Taxon 20 (5-6), 653–721.

Leites, L.P., Robinson, A.P., Rehfeldt, G.E., Marshall, J.D., Crookston, N.L., 2012. Height-growth response to climatic changes differs among populations of Douglas-fir: a novel analysis of historic data. Ecol. Appl. 22 (1), 154–165.

Martin-Benito, D., Kint, V., del Río, M., Muys, B., Cañellas, I., 2011. Growth responses of West-Mediterranean Pinus nigra to climate change are modulated by competition and productivity: Past trends and future perspectives. For. Ecol. Manage. 262, 1030–1040. https://doi.org/10.1016/j.foreco.2011.05.038.

McCullough, I.M., Davis, F.W., Williams, A.P., 2017. A range of possibilities: Assessing geographic variation in climate sensitivity of ponderosa pine using tree rings. For. Ecol. Manage. 402, 223–233. https://doi.org/10.1016/j.foreco.2017.07.025.

McGill, B.J., 2012. Trees are rarely most abundant where they grow best. J. Plant Ecol. 5 (1), 46–51. https://doi.org/10.1093/jpe/rtr036.

Milner, K.S., Coble, D.W., McMahan, A.J., Smith, E.L., 2003. FVSBGC: A hybrid of the physiological model STAND-BGC and the forest vegetation simulator. Canadian Journal of Forest Research. 33 (3), 466–479.

Mina, M., Martin-Benito, D., Bugmann, H., Cailleret, M., 2016. Forward modeling of tree-ring width improves simulation of forest growth responses to drought. Agric. For. Meteorol. 221, 13–33. https://doi.org/10.1016/j.agrformet.2016.02.005.

Monserud, R.A., 1984. Height growth and site index curves for inland Douglas-fir based on stem analysis data and forest habitat type. For. Sci. 30, 943–965.

Monserud, R.A., Sterba, H., 1996. A basal area increment model for individual trees growing in even- and uneven-aged forest stands in Austria. For. Ecol. Manage. 80 (1-3), 57–80.

Monserud, R.A., Yang, Y., Huang, S., Tchebakova, N., 2008. Potential change in lodgepole pine site index and distribution under climatic change in Alberta. Can. J. For. Res. 38, 343–352. https://doi.org/10.1139/X07-166.

Moorcroft, P.R., Hurtt, G.C., Pacala, S.W., 2001. A method for scaling vegetation dynamics: The ecosystem demography model (ED). Ecol. Monogr. 71, 557–586. https://doi.org/10.1890/0012-9615(2001)071[0557:AMFSVD]2.0.CO;2.

Moore, P.T., DeRose, R.J., Long, J.N., van Miegroet, H., 2012. Using silviculture to influence carbon sequestration in Southern Appalachian spruce-fir forests. Forests 3, 300–316. https://doi.org/10.3390/f3020300.

National Academies of Sciences, E. and M., 2019. Negative Emissions Technologies and Reliable Sequestration. National Academies Press, Washington, D.C. https://doi.org/10.17226/25259.

Pagel, J., Treurnicht, M., Bond, W.J., Kraaij, T., Nottebrock, H., Schutte-Vlok, AnneLise, Tonnabel, J., Esler, K.J., Schurr, F.M., 2020. Mismatches between demographic niches and geographic distributions are strongest in poorly dispersed and highly persistent plant species. Proc. Natl. Acad. Sci. 117 (7), 3663–3669. https://doi.org/10.1073/pnas.1908684117.

Pan, Y., Birdsey, R.A., Fang, J., Houghton, R., Kauppi, P.E., Kurz, W.A., Phillips, O.L., Shvidenko, A., Lewis, S.L., Canadell, J.G., Ciais, P., Jackson, R.B., Pacala, S.W., McGuire, A.D., Piao, S., Rautiainen, A., Sitch, S., Hayes, D., 2011. A Large and Persistent Carbon Sink in the World's Forests. Science 333 (6045), 988–993. https://doi.org/10.1126/science.1201609.

Peng, C., 2000. Growth and yield models for uneven-aged stands: past, present and future. For. Ecol. Manage. 132 (2-3), 259–279.

Pickett, S.T.A., 1989. Space-for-time substitution as an alternative to long-term studies. In: Likens, G.E. (Ed.), Long-Term Studies in Ecology: Approaches and Alternatives. Springer, New York, NY, pp. 110–135.

Piñeiro, G., Perelman, S., Guerschman, J.P., Paruelo, J.M., 2008. How to evaluate models: Observed vs. predicted or predicted vs. observed? Ecol. Modell. 216 (3-4), 316–322.

Pironon, S., Villellas, J., Thuiller, W., Eckhart, V.M., Geber, M.A., Moeller, D.A., García, M.B., 2018. The 'Hutchinsonian niche' as an assemblage of demographic

niches: implications for species geographic ranges. Ecography (Cop.) 41, 1103–1113. https://doi.org/10.1111/ecog.03414.
Pokharel, B., Froese, R.E., 2008. Evaluating alternative implementations of the Lake States FVS diameter increment model. For. Ecol. Manage. 255, 1759–1771. https://doi.org/10.1016/j.foreco.2007.11.035.
Porté, A., Bartelink, H.H., 2002. Modelling mixed forest growth: a review of models for forest management. Ecol. Modell. 150 (1-2), 141–188.
Pretzsch, H., Biber, P., 2010. Size-symmetric versus size-asymmetric competition and growth partitioning among trees in forest stands along an ecological gradient in central Europe. Can. J. For. Res. 40 (2), 370–384.
Puhlick, J.J., Weiskittel, A.R., Kenefic, L.S., Woodall, C.W., Fernandez, I.J., 2020. Strategies for enhancing long-term carbon sequestration in mixed-species, naturally regenerated Northern temperate forests. Carbon Manag. 11 (4), 381–397.
Reclamation, 2014. Downscaled CMIP3 and CMIP5 Climate and Hydrology Projections: Release of Hydrology Projections, Comparison with preceding Information, and Summary of User Needs. Denver, Colorado.
Rehfeldt, G.E., Crookston, N.L., Warwell, M.V., Evans, J.S., 2006. Empirical analyses of plant-climate relationships for the western United States. Int. J. Plant Sci. 167 (6), 1123–1150.
Rinaldi, B.N., Maxwell, R.S., Callahan, T.M., Brice, R.L., Heeter, K.J., Harley, G.L., 2021. Climate and ecological disturbance analysis of Engelmann spruce and Douglas fir in the greater Yellowstone ecosystem. Trees, For. People 3, 100053. https://doi.org/10.1016/j.tfp.2020.100053.
Running, S.W., Coughlan, J.C., 1988. A general model of forest ecosystem processes for regional applications I. Hydrologic balance, canopy gas exchange and primary production processes. Ecol. Modell. 42, 125–154. https://doi.org/10.1016/0304-3800(88)90112-3.
Sato, H., Itoh, A., Kohyama, T., 2007. SEIB-DGVM: A new Dynamic Global Vegetation Model using a spatially explicit individual-based approach. Ecol. Modell. 200, 279–307. https://doi.org/10.1016/j.ecolmodel.2006.09.006.
Scheller, R.M., Domingo, J.B., Sturtevant, B.R., Williams, J.S., Rudy, A., Gustafson, E.J., Mladenoff, D.J., 2007. Design, development, and application of LANDIS-II, a spatial landscape simulation model with flexible temporal and spatial resolution. Ecol. Modell. 201, 409–419. https://doi.org/10.1016/j.ecolmodel.2006.10.009.
Schielzeth, H., 2010. Simple means to improve the interpretability of regression coefficients. Methods Ecol. Evol. 1, 103–113. https://doi.org/10.1111/j.2041-210x.2010.00012.x.
Seidl, R., Rammer, W., Scheller, R.M., Spies, T.A., 2012. An individual-based process model to simulate landscape-scale forest ecosystem dynamics. Ecol. Modell. 231, 87–100. https://doi.org/10.1016/j.ecolmodel.2012.02.015.
Shaw, J.D., 2006. Reineke's stand density index: Where are we and where do we go from here? Soc. Am. For. 2005 Natl. Conv. 13.
Shaw, J.D., 2000. Application of Stand Density Index to Irregularly Structured Stands. West. J. Appl. For. 15, 40–42.
Shifley, S.R., He, H.S., Lischke, H., Wang, W.J., Jin, W., Gustafson, E.J., Thompson, J.R., Thompson, F.R., Dijak, W.D., Yang, J., 2017. The past and future of modeling forest dynamics: from growth and yield curves to forest landscape models. Landsc. Ecol. 32 (7), 1307–1325. https://doi.org/10.1007/s10980-017-0540-9.
Shugart, H.H., Wang, B., Fischer, R., Ma, J., Fang, J., Yan, X., Huth, A., Armstrong, A.H., 2018. Gap models and their individual-based relatives in the assessment of the consequences of global change. Environ. Res. Lett. 13 (3), 033001. https://doi.org/10.1088/1748-9326/aaaacc.
Sitch, S., Smith, B., Prentice, I.C., Arneth, A., Bondeau, A., Cramer, W., Kaplan, J.O., Levis, S., Lucht, W., Sykes, M.T., Thonicke, K., Venevsky, S., 2003. Evaluation of ecosystem dynamics, plant geography and terrestrial carbon cycling in the LPJ dynamic global vegetation model. Glob. Chang. Biol. 9 (2), 161–185.
Somerville, W., 1891. An account of Pressler's growth-borer. Bot. Soc. Edinburgh 19, 90–93.
Speer, J.H., 2010. Fundamentals of tree-ring research. University of Arizona Press, Tucson, AZ.
Stage, A.R., 1973. Prognosis model for stand development. Intermt. For. Range Exp. Station. For. Serv. US Dep, Agric, p. 137.
Stage, A.R., 1968. A tree-by-tree measure of site utilization for grand fir related to stand density index.
Swetnam, T.W., Allen, C.D., Betancourt, J.L., 1999. Applied historical ecology: Using the past to manage for the future. Ecol. Appl. 9 (4), 1189–1206.
The United States of America Nationally Determined Contribution, 2021. Reducing Greenhouse Gases in the United States: A 2030 Emissions Target.
Thuiller, W., Münkemüller, T., Schiffers, K.H., Georges, D., Dullinger, S., Eckhart, V.M., Edwards, T.C., Gravel, D., Kunstler, G., Merow, C., Moore, K., Piedallu, C., Vissault, S., Zimmermann, N.E., Zurell, D., Schurr, F.M., 2014. Does probability of occurrence relate to population dynamics? Ecography (Cop.) 37 (12), 1155–1166.
Tinkham, W.T., Mahoney, P.R., Hudak, A.T., Domke, G.M., Falkowski, M.J., Woodall, C. W., Smith, A.M.S., 2018. Applications of the United States Forest Inventory and Analysis dataset: A review and future directions. Can. J. For. Res. 48 (11), 1251–1268.
Tolwinski-Ward, S.E., Evans, M.N., Hughes, M.K., Anchukaitis, K.J., 2011. An efficient forward model of the climate controls on interannual variation in tree-ring width. Clim. Dyn. 36 (11-12), 2419–2439.
US Department of Agriculture, F.S., 2020. Forest Inventory and Analysis National Core Field Guide Volume I: Field Data Collection Procedures for Phase 2 Plots.
Walters, C., 1986. Adaptive Management of Renewable Resources. Macmillan Publishing Company, New York.
Weiskittel, A.R., Garber, S.M., Johnson, G.P., Maguire, D.A., Monserud, R.A., 2007. Annualized diameter and height growth equations for Pacific Northwest plantation-grown Douglas-fir, western hemlock, and red alder. For. Ecol. Manage. 250 (3), 266–278.
Weiskittel, A.R., Hann, D.W., Kershaw, J.A., Vanclay, J.K. (Eds.), 2011. Forest Growth and Yield Modeling. Wiley.
Zald, H.S.J., Spies, T.A., Harmon, M.E., Twery, M.J., 2016. Forest carbon calculators: A review for managers, policymakers and educators. J. For. 114 (2), 134–143. https://doi.org/10.5849/jof.15-019.
Zang, C., Biondi, F., 2015. treeclim: an R package for the numerical calibration of proxy-climate relationships. Ecography (Cop.) 38 (4), 431–436.